



**HAL**  
open science

# Intracerebral electrical stimulation of the face-selective right lateral fusiform gyrus transiently impairs face identity recognition

Angélique Volfart, Bruno Rossion, Xiaoqian Yan, Luna Angelini, Louis Maillard, Sophie Colnat-Coulbois, Jacques Jonas

## ► To cite this version:

Angélique Volfart, Bruno Rossion, Xiaoqian Yan, Luna Angelini, Louis Maillard, et al.. Intracerebral electrical stimulation of the face-selective right lateral fusiform gyrus transiently impairs face identity recognition. *Neuropsychologia*, 2023, 190, pp.108705. 10.1016/j.neuropsychologia.2023.108705 . hal-04616323

**HAL Id: hal-04616323**

**<https://hal.univ-lorraine.fr/hal-04616323>**

Submitted on 18 Jun 2024

**HAL** is a multi-disciplinary open access archive for the deposit and dissemination of scientific research documents, whether they are published or not. The documents may come from teaching and research institutions in France or abroad, or from public or private research centers.

L'archive ouverte pluridisciplinaire **HAL**, est destinée au dépôt et à la diffusion de documents scientifiques de niveau recherche, publiés ou non, émanant des établissements d'enseignement et de recherche français ou étrangers, des laboratoires publics ou privés.

# Intracerebral electrical stimulation of the face-selective right lateral fusiform gyrus transiently impairs face identity recognition

Angélique Volfart<sup>a,b,c</sup>, Bruno Rossion<sup>a,b,d</sup>, Xiaoqian Yan<sup>a,b,e</sup>, Luna Angelini<sup>a</sup>, Louis Maillard<sup>a,d</sup>,  
Sophie Colnat-Coulbois<sup>a,f</sup>, Jacques Jonas<sup>a,d</sup>

<sup>a</sup> Université de Lorraine, CNRS, F-54000 Nancy, France

<sup>b</sup> University of Louvain, Psychological Sciences Research Institute, B-1348 Louvain-La-Neuve, Belgium

<sup>c</sup> Queensland University of Technology, Faculty of Health, School of Psychology & Counselling, 4059 Brisbane, Australia

<sup>d</sup> Université de Lorraine, CHRU-Nancy, Service de Neurologie, F-54000 Nancy, France

<sup>e</sup> Fudan University, Institute of Science and Technology for Brain-Inspired Intelligence, 200433 Shanghai, China

<sup>f</sup> Université de Lorraine, CHRU-Nancy, Service de Neurochirurgie, F-54000 Nancy, France

## Corresponding Author:

### Bruno Rossion

CNRS – Université de Lorraine

Pavillon Krug, Hôpital Central, CHRU de Nancy

29 avenue du Maréchal de Lattre de Tassigny

54000 Nancy, FRANCE

+33 3 83 85 80 53

**Conflict of interest:** The authors declare no potential conflict of interest.

**Keywords:** Prosopagnosia, iEEG; direct electrical stimulation; face identity recognition; fusiform gyrus.

## **ABSTRACT**

Neuroimaging and intracranial electrophysiological studies have consistently shown the largest and most consistent face-selective neural activity in the middle portion of the human right lateral fusiform gyrus ('fusiform face area(s), FFA). Yet, direct evidence for the critical role of this region in face identity recognition (FIR) is still lacking. Here we report the first evidence of transient behavioral impairment of FIR during focal electrical stimulation of the right FFA. Upon stimulation of an electrode contact within this region, subject CJ, who shows typical FIR ability outside of stimulation, was transiently unable to point to pictures of famous faces among strangers and to match pictures of famous or unfamiliar faces presented simultaneously for their identity. Her performance at comparable tasks with other visual materials (written names, pictures of buildings) remained unaffected by stimulation at the same location. During right FFA stimulation, CJ consistently reported that simultaneously presented faces appeared as being the same identity, with little or no distortion of the spatial face configuration. Independent electrophysiological recordings showed the largest neural face-selective and face identity activity at the critical electrode contacts. Altogether, this extensive multimodal case report supports the causal role of the right FFA in FIR.

## 1. INTRODUCTION

The ability to recognize the identity of people from their faces is a key function of the human brain that subtends most of our daily social interactions. The neural basis of human face identity recognition (FIR) has been extensively investigated but remains incomplete and debated. Lesion studies of neurological patients with FIR impairment – often reported as cases of prosopagnosia - have most consistently identified brain damage in regions of the ventral occipito-temporal cortex (VOTC), with a right hemispheric dominance ([Meadows 1974](#); [Bouvier and Engel 2006](#); [Barton 2008](#); [Tranel et al. 2009](#); [Cohen et al. 2019](#)). Neuroimaging and intracranial EEG studies have showed an extensive bilateral VOTC network of regions responding preferentially to faces over non-face objects (i.e., face-selective regions), also with a right hemispheric dominance ([Grill-Spector et al. 2017](#); [Rossion et al. 2018 for reviews](#)). Within this network, the lateral portion of the right middle fusiform gyrus (LatMidFG), a hominoid-specific structure ([Bryant and Preuss 2018](#)), shows the highest and most consistent face-selective signal in neuroimaging (i.e., the so-called “Fusiform Face Area”, FFA, or pFus-faces and mFus-Faces; [Kanwisher et al. 1997](#); [Kanwisher and Yovel 2006](#); [Rossion et al. 2012](#); [Zhen et al. 2015](#); [Grill-Spector et al. 2017](#); [Gao et al. 2018](#); [Chen et al. 2022](#)) and intracranial EEG studies ([Jonas et al. 2016](#); [Jacques et al. 2022](#)).

Neuroimaging studies measuring repetition suppression (or adaptation) effects for (usually unfamiliar) pictures of facial identities have reported significant effects in the face-selective LatMidFG (i.e., FFA), sometimes with a right hemispheric predominance ([Gauthier et al. 2000](#); [Schultz and Rossion 2006](#); [Gilaie-Dotan et al. 2010](#); [Ewbank et al. 2013](#); [Hermann et al. 2017](#); [Hughes et al. 2019](#)). A recent large-scale intracranial EEG study found individual unfamiliar face discrimination responses largely distributed across the bilateral VOTC, with the largest activity in the right LatMidFG ([Jacques et al. 2020](#)). However, these studies supporting the role of the (right) face-selective LatMidFG in FIR cannot inform on the *causal* role of this region for this function. Interestingly, while the right LatMidFG is often damaged in reported

cases of prosopagnosia, it is also entirely spared in many cases (e.g., [Rossion, Caldara, et al. 2003](#); [Bouvier and Engel 2006](#); e.g., 15 cases out of 44 in [Cohen et al. 2019](#)).

Direct electrical stimulation (DES) performed in epileptic patients implanted with intracranial electrodes for clinical reasons can temporarily disrupt the function(s) of a stimulated brain region, allowing to observe behavioral consequences in real-time ([Jonas and Rossion 2023](#)). Early studies reported disruption of famous face naming during VOTC stimulation in several individuals, albeit with a left hemispheric dominance and no specific localization relative to fMRI-defined face-selectivity ([Allison et al. 1994](#); [Puce et al. 1999](#)). Over the last decade, DES studies targeting specifically the right LatMidFG have reported face-related perceptual changes, i.e., changes in the phenomenological experience of the face stimulus, usually the experimenter's face in front of the patient or a presented picture ([Parvizi et al. 2012](#); [Rangarajan et al. 2014](#); [Schalk et al. 2017](#); [Jonas et al. 2018](#); [Schrouff et al. 2020](#); [Sanada et al. 2021](#); see also [Mundel et al. 2003](#)). However, to date, while several cases of behavioral FIR impairment have been reported upon stimulation of other right hemispheric VOTC face-selective regions (i.e., in the inferior occipital gyrus: [Jonas et al. 2012, 2014](#); the anterior fusiform gyrus: [Jonas et al. 2015](#); [Volfart et al. 2022](#)), no objective (i.e., behavioral) FIR impairment has been reported upon intracranial stimulation of the (right) LatMidFG (see the review of [Jonas and Rossion 2021](#)). As a matter of fact, the well-known case of [Parvizi et al. \(2012\)](#), who experienced spectacular perceptual distortion of the spatial configuration of presented faces ('metamorphopsia'), showed no effect of DES on behavioral performance at naming pictures of celebrities during right FFA stimulation.

Here we report the case of subject CJ in which DES of the face-selective right LatMidFG (i.e., FFA) elicits a transient FIR impairment, filling a gap in the scientific literature and providing original evidence for the causal role of this region in FIR. In terms of subjective reports, CJ, documented with typical FIR ability outside of stimulation, consistently reported that "*all presented faces looked the same*" upon focal right LatMidFG stimulation. Her impairment, including its specificity to faces, is objectively quantified with a variety of behavioral tasks

including famous face and unfamiliar face matching, and famous face pointing among distractors. Complementary fMRI recordings, as well as face-selective, unfamiliar face discrimination and famous face identity electrophysiological measures on the critical contacts altogether provide unique evidence for a critical role of the right LatMidFG in human FIR.

## **2. MATERIALS AND METHODS**

Note that with the exception of the localization of implanted electrodes, the methodology described below has been fully described recently in another recent case study with stimulation applied to a different brain region, i.e., the right anterior fusiform gyrus ([Volfart et al. 2022](#)).

### **2.1 Case description**

The subject is a right-handed 43-year-old woman (CJ) with refractory focal epilepsy. She underwent SEEG in May 2019 as part of the clinical investigation for her epilepsy. Following SEEG exploration, two independent epileptic foci were found in right and left medial temporal lobes and therefore subject CJ was contraindicated for a resection surgery.

Patient CJ gave written consent for the experimental procedures that were administered during her SEEG exploration and that were part of the clinical investigation (REUNIE, trial N° 2015-A01951-48, approved by the local ethical committee CPP Est III, N°16.02.01). She also gave written consent for the fMRI experiment and the use of video material.

### **2.2 Neuropsychological assessment**

#### **2.2.1 General assessment**

Subject CJ had a general intellectual efficiency in the high average (total IQ: 119; WAIS-IV, [Wechsler 2008](#)). Her neuropsychological assessment showed normal performance in naming (DO80 naming test, [Deloche and Hannequin 1997](#)), processing speed (subtest Code, WAIS-IV) and short-term memory (subtest Digit span, WAIS-IV). In line with the location of her epileptogenic foci in the medial temporal lobes, she had below normal performance in learning and retrieving verbal information from memory (French adaptation from the Buschke Selective

Reminding Test, [Buschke 1973](#); [Rectem et al. 2004](#)). However, she had normal performance with non-verbal information (Brief Visuospatial Memory Test-Revised, [Benedict 1997](#)). CJ never complained of FIR difficulties in daily life, nor during or after epileptic seizures.

### **2.2.2 Face identity recognition**

We conducted a series of behavioral tests outside the SEEG procedure to specifically assess the performance of CJ in face/object recognition. These tests included: (1) the Benton Facial Recognition Test (BFRT: [Benton et al. 1983](#); electronic version, BFRT-c: [Rossion and Michel 2018](#)) in which the participant has to match a target face with other images of the same face varying in lighting and head orientation (all images are presented simultaneously); (2) a face and car delayed matching task at upright and inverted orientations (experiment 4 in [Busigny and Rossion 2010](#)) in which the participant is first presented with a target face or car picture and then with two face or car probes, and is asked to indicate which of two probes is the same exemplar as the target; (3) a famous and unfamiliar face simultaneous matching task at upright and inverted orientations in which the participant is shown a famous or unfamiliar face picture at the top of the screen and two famous or unfamiliar probes below, and is asked to indicate which of the probes on the bottom is the same as the target face; (4) a face memory task (administered immediately after the famous and unfamiliar face matching task) in which the participant is presented with two faces on the screen (one of them corresponding to a face that was presented in the face matching task), and is asked to indicate which of the two faces was previously seen; (5) a famous face pointing task in which the participant sees three faces in a row (one of these faces is famous while the two others are unfamiliar distractors), and has to indicate which face is famous; (6) a famous name pointing task, a task similar to the famous face pointing task, except that a famous name and two unfamiliar fictional names are presented instead of faces (see all methods in [Supplementary Information](#)). All tasks were administered through E-Prime 2.0 on a 60 Hz screen, at a distance of about 60 cm. Five control participants (matched on gender, age, handedness and educational level) performed the same tests. To compare the results of CJ to the control participants, we used the modified t-test of

Crawford and Howell for single-case studies ([Crawford and Howell 1998](#)) with a p value < 0.05 (one-tailed) considered as statistically significant.

The results are shown in **Supplementary Table S1**. CJ performed in the normal range at all identity matching tasks with upright faces (and non-face objects), both in accuracy and response times (RT). At the BFRT-c, she scored in the normal range (>41) although there was a non-significant trend towards a lower score than the controls tested here (42 vs.  $48.2 \pm 2.8$ ;  $p = 0.057$ ). However, CJ was numerically faster than average to perform the test (234s vs.  $363s \pm 128$ ;  $p = 0.205$ ) so that and her inverse efficiency score (RT/Acc) did not differ from controls ( $5.6$  vs.  $7.5 \pm 2.7$ ;  $p = 0.278$ ).

### **2.3 Stereotaxic placement of intracerebral electrodes**

Intracerebral electrodes (Dixi Medical, Besançon, France) were stereotaxically implanted into CJ's brain in order to delineate the seizure onset zone ([Talairach and Bancaud 1973](#)). The implantation procedure is detailed in [Salado et al. \(2017\)](#). The sites of electrode implantation were determined based on non-invasive clinical data collected during an earlier phase of the investigation. Fifteen electrodes were implanted in total, targeting both the left and right temporal lobes (7 in the left, 8 in the right). Thirteen standard electrodes had macro-contacts only (DixiMedical, Besançon, France), and two electrodes were macro-micro electrodes, i.e., electrodes with macro-contacts modified to include microwires at their end (Ad-Tech, Oak Creek, USA). Electrode F (macro-micro electrode) targeted the right LatMidFG (**Figure 1**). There was no electrode implanted in the LatMidFG of the left hemisphere. This article will focus on stimulations and recordings performed with macro-contacts only (n=147 implanted in total).

The SEEG signal was recorded at a 2 kHz sampling rate on a 256-channel amplifier (Cervello, Blackrock Microsystems, USA). The reference electrode during data acquisition was a midline prefrontal scalp electrode (Fpz).



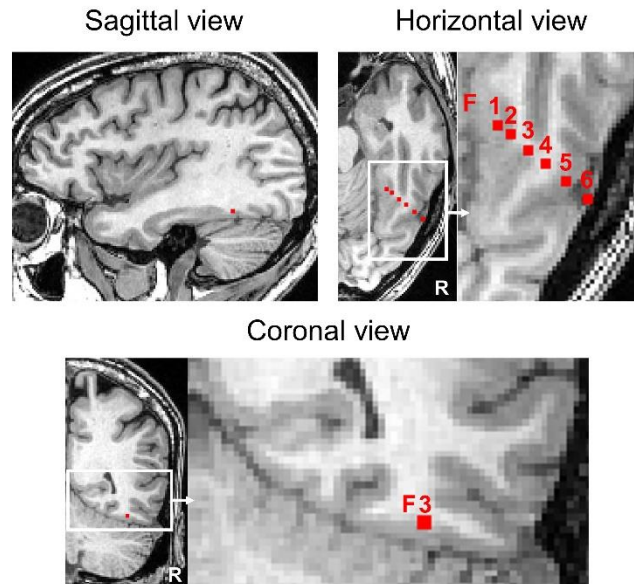


**Figure 1.** Anatomical location of electrode *F* (in red) in sagittal, horizontal and coronal MRI slices.

## 2.4 Intracranial electrical stimulations

### 2.4.1 General procedure

Intracerebral electrical stimulations were applied at 1.2 mA between two adjacent contacts of electrode *F* as biphasic square wave electrical pulses with 1050  $\mu$ s width (alternating positive and negative 500  $\mu$ s phases, spaced from each other by 25  $\mu$ s) delivered at 55 Hz during 5 s (except for 7 out of 47 stimulation sessions, see below). These stimulation parameters are typical in SEEG (Trébuchon and Chauvel 2016; Isnard et al. 2018; Ritaccio et al. 2018; So and Alwaki 2018; Grande et al. 2020; Aron et al. 2021) and were also used in our previous reports eliciting transient FIR impairments (Jonas et al. 2012, 2015, 2018; Volfart et al. 2022). CJ was not aware of the exact stimulation onset, duration and termination (no pain during stimulation, no click sound at onset, etc.). She was never made aware of the stimulation site or the nature of the impairments that could be potentially elicited during electrical stimulations. The neurologist (JJ) performed all electrical stimulations and set the stimulation site, the stimulation parameters, the task, and stimulation the onset of the stimulation. Several

experimenters were present in the patient's room during stimulation, including authors AV and BR.

During electrical stimulation sessions, CJ was asked to perform several types of behavioral tasks involving images of faces, objects, buildings and written names: pointing to famous faces and names (**Figure 2A**), naming famous faces and buildings, and matching famous or unfamiliar faces for their identity (**Figure 2B**). Considering the limited amount of testing time afforded by the clinical context, we first identified the relevant electrode contacts for FIR using one task (pointing to a famous face among three choices, i.e., famous face pointing task) and then further tested these contacts with the remaining tasks. Since we found a FIR impairment with the famous face pointing task when stimulating the first electrode tested, i.e., electrode F, we focused on this electrode to maximize the number of relevant tasks and trials.

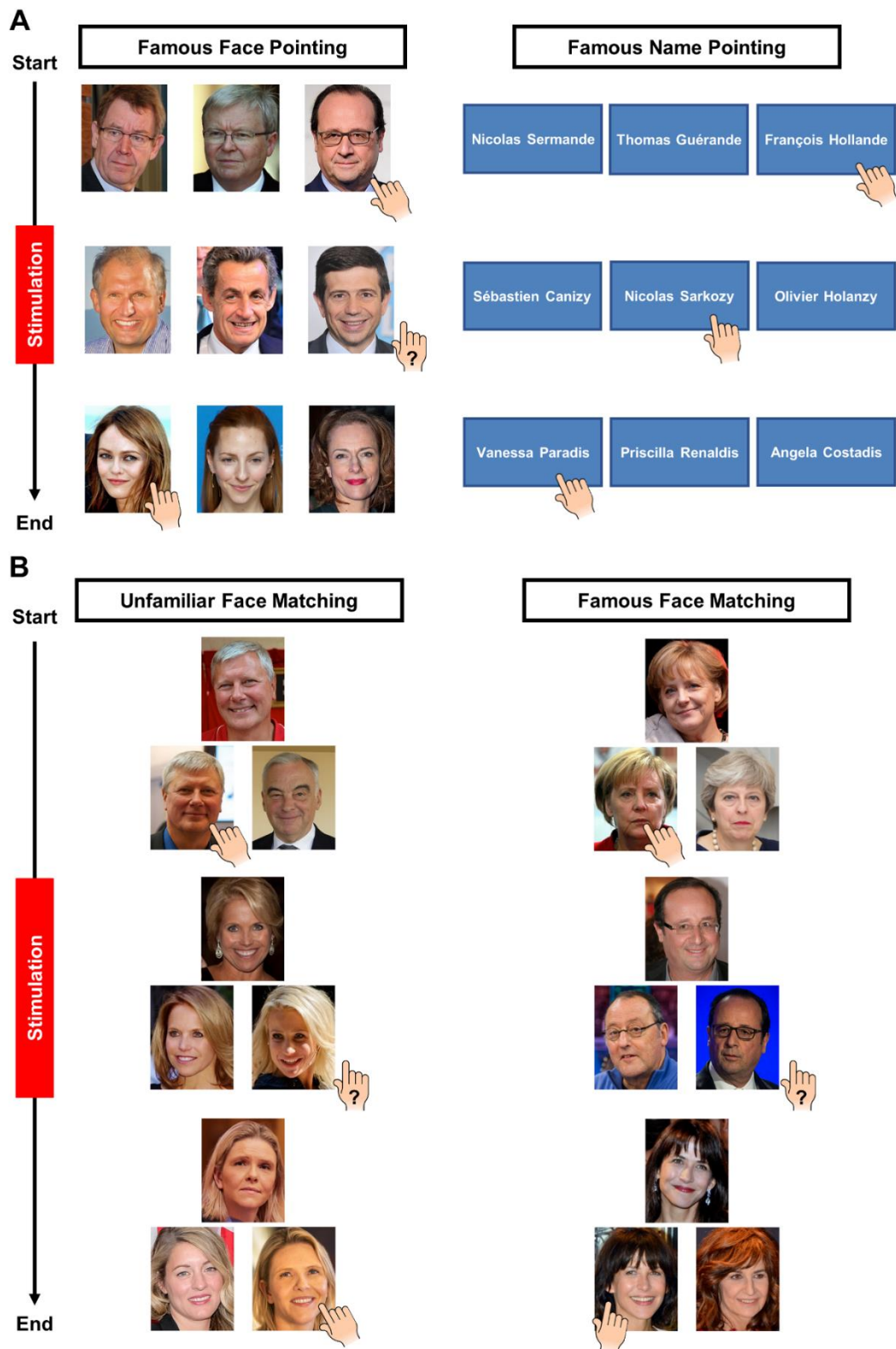


**Figure 2. A.** Schematic representation of the stimulation procedure for the famous face and name pointing tasks performed during electrical stimulation (see also [Volfart et al. 2022](#), in which the same tasks were used in another case study). A trial consisted in 3 pictures of faces or written names presented next to each other, with always one famous and two unfamiliar

identities. CJ had to point to the famous item, before, during (5 s) and after the electrical stimulation of two adjacent intracerebral contacts. Here an error is illustrated during stimulation, with correct performances before and after stimulation. Note that there was often more than one trial presented before, during and after stimulation (**Supplementary Table S2**).

**B.** Schematic representation of the stimulation procedure for the famous and unfamiliar face matching tasks performed during electrical stimulation. Each trial consisted of three face photographs organized in two rows, with a target on top and two probes on the bottom: one being another picture of the target identity and the other one being a picture of another identity. CJ had to point to the probe matching the face on top, before, during and after the electrical stimulation of two adjacent intracerebral contacts. Again, there was often more than one trial presented before, during and after stimulation (**Table S2**). Note that the pictures used in this figure were not those used in the original paradigm for copyright reasons (copyright information for the pictures shown here are available in **Supplementary Information**).

The stimulation sites, the number of stimulation sessions performed at each stimulation site and type of task used will be presented in the results section. Below, we describe the different face and non-face tasks performed during stimulation sessions. For each stimulation and task, we measured accuracy before, during and after stimulation both online and retrospectively with the video recordings. A trial was considered as failed if CJ either produced an erroneous response or did not reply. To assess a significant effect of the stimulation, we compared accuracy rates during stimulation time versus accuracy rates outside of stimulation (i.e., before and after stimulation) across stimulation sessions for each site and each task using chi square tests ( $p < 0.05$ ).

#### **2.4.2 Famous face and famous name pointing tasks**

These tasks were the same as those used outside the SEEG procedure (see Neuropsychological assessment section). They have been described and used in a previous case (DN) of transient FIR impairment with stimulation in the right anterior fusiform gyrus (Volfart et al. 2022) and validated in a well-known case of prosopagnosia (PS; see Rossion 2022). During the neuropsychological assessment, CJ's accuracy at these two tasks was 100% (**Table S1**).

The trials consisted in 3 faces or written names presented side-by-side, with always one famous identity and two unfamiliar identities (**Figure 2A; Video S1**). The famous identity was the same across categories (faces and names). The unfamiliar identities were either faces of foreign famous identities not known by French people or phonologically-similar fictional names. Face images were 5.7 cm wide by 7.7 cm high; written names ranged from 2.1 to 5.6 cm in width, and from 0.4 to 1.3 cm in height. For each stimulation session, the subject was presented with a set of 6 to 10 trials of the same category (faces or names), presented one by one (leading to, e.g., a total of 22 trials, 7+6+9, for stimulation of F1-F2 during the famous face pointing task, across 3 sessions; see **Results section**). CJ had to point to the famous face or name in turn.

In total, CJ was presented with 122 face trials (across 16 stimulation sessions): 37 before, 39 during and 46 after electrical stimulation (since the stimulus set consisted in 50 different face trials, several face trials were repeated across stimulation sessions). CJ was also presented with 34 name trials (across 5 stimulation sessions): 14 before, 16 during and 4 after electrical stimulation.

Immediately after 5 stimulation sessions that elicited a FIR impairment (out of 7: 1 on F1-F2, 2 on F2-F3 and 2 on F3-F4), the subject was presented with the missed trials (no response or error) and asked to perform the task again (**Video S1**). These trials were not included in any analysis.

Note that 5 stimulation sessions with the face pointing task were performed with different stimulation settings (1 mA instead of 1.2 mA).

### **2.4.3 Famous and unfamiliar face matching tasks**

This task was the same as the famous and unfamiliar face simultaneous matching task administered during neuropsychological assessment before the SEEG procedure, except that only upright faces were presented. CJ's performance at this task during the neuropsychological assessment was 95.5% for famous faces and 100% for unfamiliar faces (**Table S1**). Each trial consisted of three face photographs organized in two rows, with a target on top and two probes below, one of the probes being another photograph of the target identity and the other probe being a photograph of another identity (**Figure 2B; Videos S2 and S3**). Face images were 7 cm wide by 9 cm high. CJ had to match the probe with the target by pointing to the correct face. For each stimulation session, CJ was presented with 6 to 9 trials from the same category (famous faces or unfamiliar faces), presented one by one.

### **2.4.4 Famous face and famous building naming**

Stimulations were also carried out during recognition of sets of images of the same category presented one by one (famous faces or famous buildings). CJ had to name each image in turn. Face images were 13.4 cm wide by 15 cm high; famous building images measured between 9.3 and 15.7 cm wide, and between 9.8 and 12.5 cm high. For each stimulation session, the subject was presented with a set of 1 to 9 trials of the same category (faces or buildings), presented one by one.

In total (across 6 stimulation sessions with faces and 4 with buildings), the subject was presented with 29 famous faces (10 during electrical stimulation, 14 before and 5 after) and 22 famous buildings (8 during, 7 before and 7 after). Given that the famous face and the famous building sets consisted in 50 and 14 items, respectively, some items were repeated across stimulation sessions. Note that two stimulation sessions with the famous face naming task were performed with different stimulation parameters (1 mA for 10 s instead of 1.2 mA for 5 s).

## 2.5 Fast periodic visual stimulation: intracerebral responses

### 2.5.1 FPVS paradigms: stimuli and procedure

Well-validated fast periodic visual stimulation (FPVS) (or “frequency-tagging”; see [Norcia et al. 2015](#); [Rossion et al. 2020](#)) paradigms were used to identify face-selective contacts and contacts sensitive to unfamiliar face discrimination and famous face identity recognition (**Figure 3**, see also **Supplementary Information** for all methodological details).

Face-selective neural activity was recorded with 70-seconds sequences of variable non-face object images presented at 6 Hz while inserting periodically (every 5 images; i.e., 1.2 Hz) widely variable natural images of face stimuli (Face Categorization experiment, **Figure 3A**). This paradigm was run exactly as in intracerebral recording group studies (e.g., [Jonas et al. 2016](#); [Hagen et al. 2020](#)). Unfamiliar face discrimination neural activity was recorded with a paradigm presenting the same unfamiliar face identity at a fast 6 Hz rate while periodically inserting (every 9 images; i.e., 0.666 Hz) different unfamiliar face identities (Unfamiliar Face Discrimination experiment; [Liu-Shuang et al. 2014a](#); [Rossion et al. 2020](#); **Figure 3B**). Faces were presented either at upright or inverted orientation in separate sequences as in [Jacques et al. 2020](#), except for the periodicity of identity change (1/9 instead of 1/5). Finally, responses reflecting sensitivity to famous face identity were recorded by presenting variable images of unfamiliar faces also at 6 Hz, with different exemplars of the same famous identity appearing every 9 stimuli (0.666 Hz) (Famous Face Identity experiment; [Zimmermann et al. 2019](#); **Figure 3C**). During these FPVS paradigms, CJ fixated a small black cross presented continuously at the center of the stimuli and had to detect brief color-changes of this fixation cross, so that neural responses were measured without explicit task.

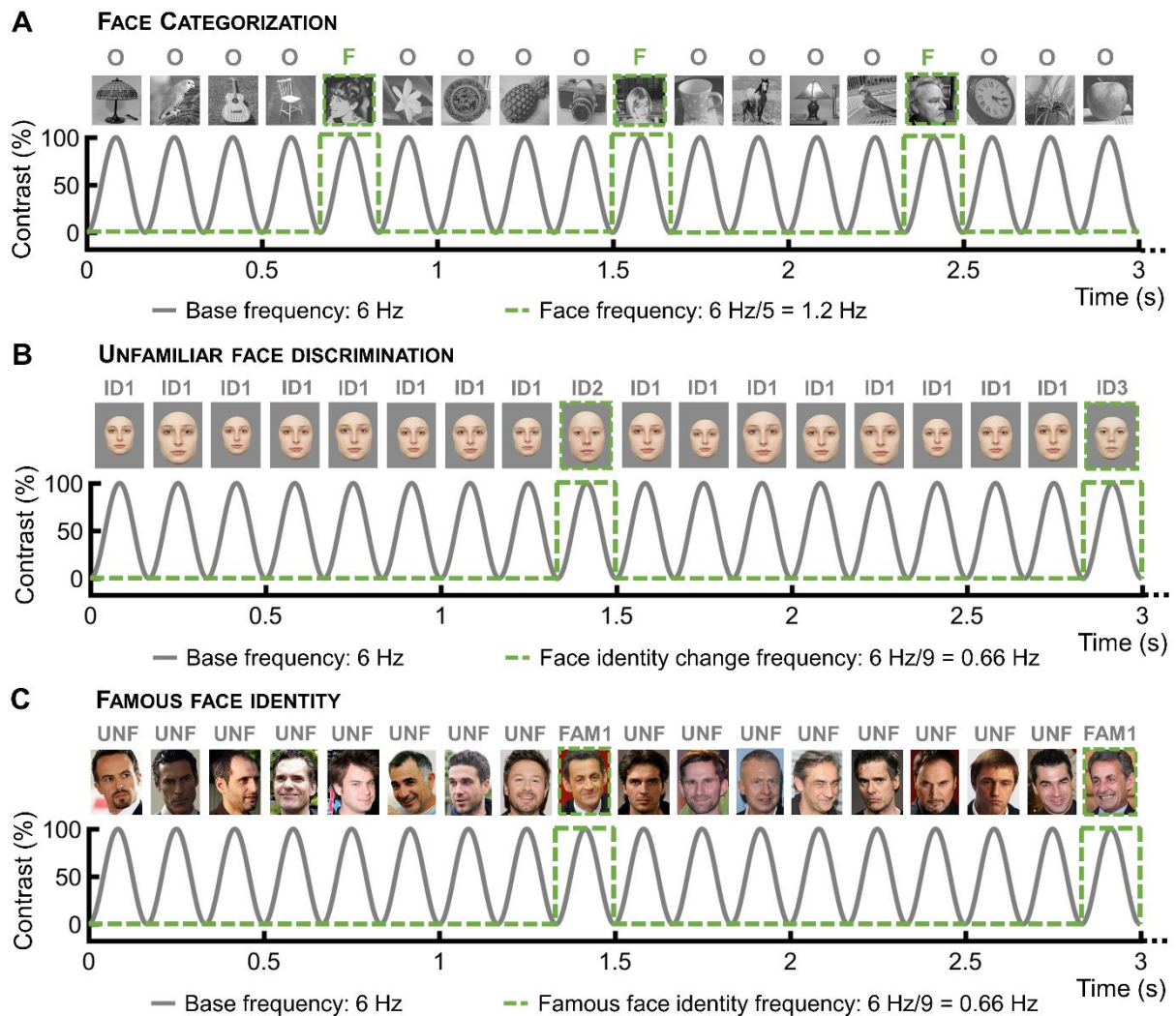


**Figure 3. FPVS experiments. A.** Face Categorization paradigm used to define face-selective neural activity (Rossion et al. 2015). Natural images of objects are presented at 6 Hz with sinusoidal contrast-modulation. Face images appear every 5 stimuli, so that the face-selective frequency is 1.2 Hz (i.e., 6 Hz / 5). **B.** Unfamiliar Face Discrimination paradigm used to measure sensitivity to unfamiliar face individuation (Liu-Shuang et al. 2014; Rossion et al. 2020). Cropped images of the same unfamiliar face identity, randomly varying in size, are presented at 6 Hz. Different unfamiliar face identities are inserted every 9 stimuli (frequency of identity change of 0.666 Hz, i.e., 6 Hz / 9). Faces were presented either at upright or inverted orientation in separate sequences. **C.** Famous Face Identity paradigm used to measure sensitivity to individual famous faces (Zimmermann et al. 2019). Natural images of unfamiliar faces are presented at 6 Hz. Different images of a single famous identity appear every 9<sup>th</sup> stimulus (in this example, the former French president, Nicolas Sarkozy), at a frequency of 0.666 Hz.



### **2.5.2 Frequency-domain analyses in the low-frequency bands**

**Preprocessing.** Analyses were carried out using *Letswave 5*, with a similar procedure as in recent reports (e.g., [Lochy et al. 2018](#); [Hagen et al. 2020](#); [Jacques et al. 2020](#); [Volfart et al. 2022](#)). Portions of SEEG recordings corresponding to FPVS sequences were extracted using segments exceeding the actual visual presentation length (74-second segments, -2 s to +72 s). These segments were then cropped to an integer number of cycles beginning after the 2 s fade-in and ending before the 2 s fade-out (Face Categorization = 131,666 bins; Unfamiliar Face Discrimination = 129,012 bins; Famous Face Identity = 129,012 bins). Sequences corresponding to the same condition were averaged in the time domain. A Fast Fourier Transform (FFT) was then applied to these averaged segments and amplitude spectra were extracted for all contacts.

**Identification of significant responses in the low-frequency bands.** Face-selective, unfamiliar face discrimination or famous face identity responses significantly above noise level at the oddball stimulation frequency and its harmonics were determined in each condition as follows: (1) the FFT spectrum was cut into segments of 1 Hz centered at the target response frequencies (i.e., 1.2 Hz for the Face Categorization paradigm, 0.666 Hz for the Unfamiliar Face Discrimination and Famous Face Identity paradigms) and harmonics, until the last harmonic before 6 Hz base frequency: 4 harmonics for the Face Categorization paradigm (as in [Jonas et al. 2016](#); [Hagen et al. 2020](#)), 8 harmonics for the Unfamiliar Face Discrimination and Famous Face Identity paradigms; (2) the amplitude values of these FFT segments were summed ([Retter and Rossion 2016](#); [Retter et al. 2021](#)); (3) the summed FFT spectrum was transformed into a Z-score by computing the difference between the amplitude at the target frequency bin and the mean amplitude of 48 surrounding bins (25 bins on each side, i.e., 50 bins, excluding the first bin directly adjacent to the bin of interest, i.e. 48 bins) divided by the standard deviation of amplitudes in the corresponding 48 surrounding bins (see also [Lochy et al. 2018](#)). A contact was considered as showing a significant response in a given condition if the Z-score at the target frequency bin exceeded 3.1 (i.e.,  $p < 0.001$ ).

**Quantification of responses amplitude in the low-frequency bands.** Baseline-corrected amplitudes in microvolts ( $\mu\text{V}$ ) were computed as the difference between the amplitude at each frequency bin and the average of 48 corresponding surrounding bins (25 bins on each side, i.e., 50 bins, but excluding the 2 bins directly adjacent to the bin of interest, i.e., 48 bins). The target responses were then quantified at each contact as the sum of the baseline-subtracted amplitude across harmonics (Retter and Rossion 2016). The range over which frequency harmonics were summed extended from the 1st until the 14th harmonics (from 1.2 to 16.8 Hz) for the Face Categorization paradigm, excluding the 5th and 10<sup>th</sup> harmonics that coincided with the base frequency (Jonas et al. 2016; Hagen et al. 2020), and from the 1st to the 10th (from 0.666 to 6.666 Hz), excluding the 9<sup>th</sup> harmonic that coincided with the base frequency (the 10<sup>th</sup> harmonic corresponded to the last consecutive harmonic with a Z score  $> 3.1$  across all contacts implanted in CJ's brain for these two paradigms) for the Unfamiliar Face Discrimination and Famous Face Identity paradigms.

**Statistical comparison between upright and inverted response amplitudes.** For the Unfamiliar Face Discrimination, we statistically compared the amplitudes of the target responses at the upright and inverted conditions on each contact. To do so, the upright and inverted summed FFT segments were subtracted from one another (upright – inverted) and transformed into a Z-score. A contact was considered as showing a larger amplitude at the upright than in the inverted condition if the Z-score at the target frequency bin exceeded 3.1 (i.e.,  $p < 0.001$ , one-tailed: upright>inverted).

### **2.5.3 Frequency-domain analyses in the high-frequency bands (“gamma activity”)**

Even though face-selective neural responses in low- and high-frequency bands largely overlap spatially (Jacques et al. 2022), we also examined these responses in high-frequency broadband activity (i.e., between 30 and 160 Hz, “gamma activity”) which are thought to reflect population-level neuronal firing, to correlate with BOLD activity and to reflect more local neural activity (e.g., Niessing et al. 2005; Hermes et al. 2012; see also Jacques et al. 2022). Event-

related spectral perturbations (ERSP) were computed using *Letswave 5* similarly to what was reported in [Jacques et al. 2022](#). Variation in signal amplitude as a function of time and frequency was estimated by a Morlet wavelet transform on each SEEG segment from frequencies of 1 to 160 Hz, in 2 Hz increments. The number of cycles (i.e., central frequency) of the wavelet was adapted as a function of frequency from 2 cycles at the lowest frequency to 9 cycles at the highest frequency. The wavelet transform was computed on each time-sample and the resulting amplitude envelope was downsampled by a factor of 12 (i.e., to a 166.6 Hz sampling rate). Amplitude was normalized across time and frequency to obtain the percentage of power change generated by the stimulus onset relative to the mean power in a pre-stimulus time-window (-1600 ms to -300 ms relative to the onset of the stimulation sequence). Then, the amplitude was averaged across frequencies (between 30 Hz and 160 Hz), the high-frequency broadband envelopes corresponding to the same condition were averaged in the time domain, and the frequency content of the high-frequency broadband envelope was transformed using a Fast Fourier transform.

Significant responses in the high-frequency bands were detected similarly as for the low-frequency bands: (1) the FFT spectrum was cut into 1 Hz segments centered at the target response frequencies (i.e., 1.2 Hz) and 4 harmonics; (2) the amplitude values of these FFT segments were summed; (3) the summed FFT spectrum was transformed into a Z-score. Z-scores were computed as the difference between the amplitude at the oddball frequency bin and the mean amplitude of 48 surrounding bins (25 bins on each side, i.e., 50 bins, excluding the first bin directly adjacent to the bin of interest, i.e., 48 bins) divided by the standard deviation of amplitudes in the corresponding 48 surrounding bins. A contact was considered as showing a significant face-selective response if the Z-score at the target frequency bin exceeded 3.1 (i.e.,  $p < 0.001$ ).

The quantification of amplitudes was done similarly as for responses in the low-frequency bands, i.e., summing amplitudes from the 1<sup>st</sup> to the 12<sup>th</sup> harmonic (excluding the 5<sup>th</sup> and 10<sup>th</sup> harmonics that coincided with the base frequency).

## 2.6 Face-selectivity: fMRI

We localized face-selective regions with a Fast Periodic Stimulation fMRI paradigm (Gao et al. 2018, see **Supplementary Information**), which provides with identification of the same regions as conventional fMRI paradigms with substantial advantages in sensitivity, specificity and objectivity of definition of face-selective neural responses (Gao et al. 2018, see also Gao et al. 2022). CJ was tested with fMRI about two months after the SEEG procedure. Natural non-face object images were presented at a fixed rate of 6 Hz (i.e., 6 images by second). Mini face “bursts” with a duration of 2.167 s were embedded every 9 s (i.e.,  $1/9 = 0.111$  Hz). Each burst consisted of a set of seven natural face images interleaved with six object to avoid potential neural adaptations to consecutive face images. The face burst created direct contrast between face and non-face objects. Therefore, a neural response measured exactly at 0.111 Hz reflects a selective and reliable response to the face stimuli. Each fMRI sequence (run) lasted 426 s of 44 cycles of mini face burst appearing at every 9 s (including a 15 s baseline). CJ was tested with two functional localizer runs. To measure the magnitude of the face-selective responses at the stimulation frequency of 0.111 Hz, we extracted the amplitude spectrum from the preprocessed BOLD time series with a Fast Fourier Transform (FFT) (see **Supplementary Information**, and all methods as in Gao et al. 2018).

For result visualization, the functional activation map was coregistered to the high-resolution T1-weighted image (AC-PC plane aligned) using SPM (<https://www.fil.ion.ucl.ac.uk/spm/>). To assess the spatial relationship between face-selective activations and intracerebral electrodes, we further extracted the electrode contact coordinates by fusing the T1-weighted image with the post-operative CT-scan.

## 3. RESULTS

### 3.1 Overview of the experimental plan

In subject CJ, intracerebral electrical stimulations were applied between two adjacent intracerebral contacts while she was tested with a set of various tasks, including a famous face

pointing task (and its famous name counterpart) and famous or unfamiliar face matching tasks that did not require any verbal output (**Figure 2A and B**). Importantly, outside the SEEG procedure, CJ's performance on all these pointing/matching tasks was at, or close to, ceiling (95% to 100%, **Table S1**).

Considering the limited amount of time afforded by the clinical context, we first identified the relevant electrode contacts for FIR with the famous face pointing task (which allows to test CJ's FIR ability without requiring any verbal output) and then further tested these contacts with the remaining tasks. Since we found a FIR impairment when stimulating the first electrode tested, i.e., electrode F (**Figure 1**), we focused on this electrode to maximize the number of tasks and trials. Independently of the electrical stimulation sessions, we identified face-selective contacts and contacts sensitive to unfamiliar face discrimination and famous FIR using well-validated FPVS paradigms during SEEG recordings (**Figure 3**, see also **Supplementary Information** for all methods details). Finally, we localized face-selective regions in fMRI with a Fast Periodic Stimulation fMRI paradigm performed two months after the SEEG procedure.

### **3.2 Stimulating the right lateral fusiform gyrus elicits transient FIR impairment**

The stimulations sites, the number of stimulation sessions performed at each stimulation site and type of task used are presented in **Figure 4** (see also **Table S2**). Reproducible transient FIR impairments were elicited when electrical stimulation involved the right LatMidFG across multiple stimulation sessions and tasks (bipolar stimulations of contacts F1-F2, F2-F3 and F3-F4; Talairach coordinates: x: 30 to 37, y: -41 to -47, z: -14.9; **Figures 4 and 5A; Table S2**).

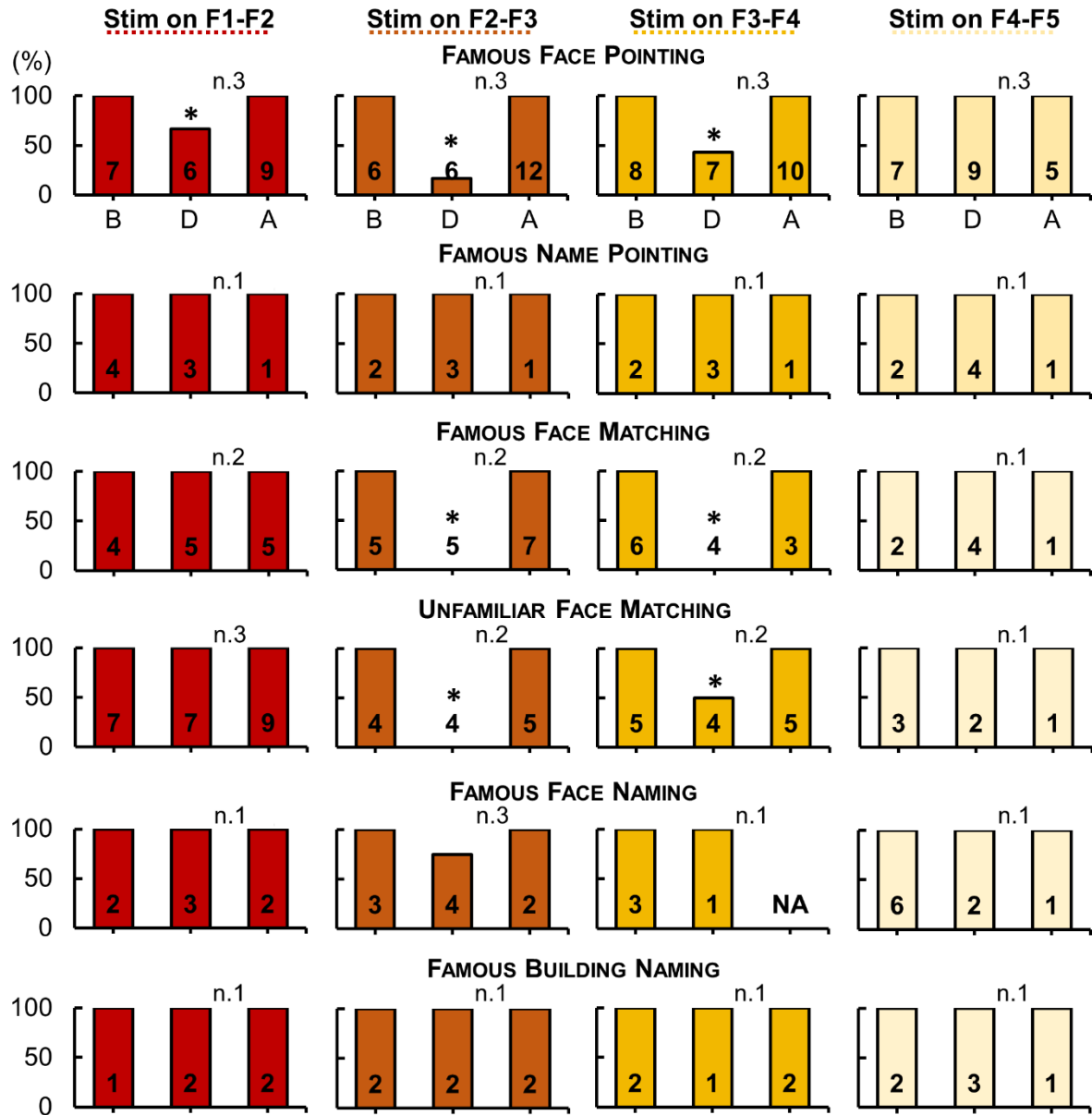


**Figure 4.** Summary of the behavioral results obtained during electrical stimulation performed in CJ's right fusiform gyrus. For each stimulation site and task, the number of stimulation sessions (e.g., top left: 3 stimulations, i.e., n.3), as well as the number of trials across stimulations before (B), during (D) and after (A) stimulation, are indicated (e.g., top left: 7 trials before stimulation on F1-F2, 6 during stimulation, and 9 after stimulation; two trials were failed during stimulation, i.e., 4/6 performance, so the accuracy decreased to 66.6% during stimulation). The asterisks indicate a significant accuracy difference between the stimulation period and outside stimulation (before and after periods merged together) as assessed by chi square tests. Note that during the famous face naming tasks, CJ's performance was close to normal (1 error only for F2-3 stimulation), but she experienced

substantial changes of the face percept in two trials in which she provided a correct answer (one on F2-3 and one on F3-4 stimulation; see main text).

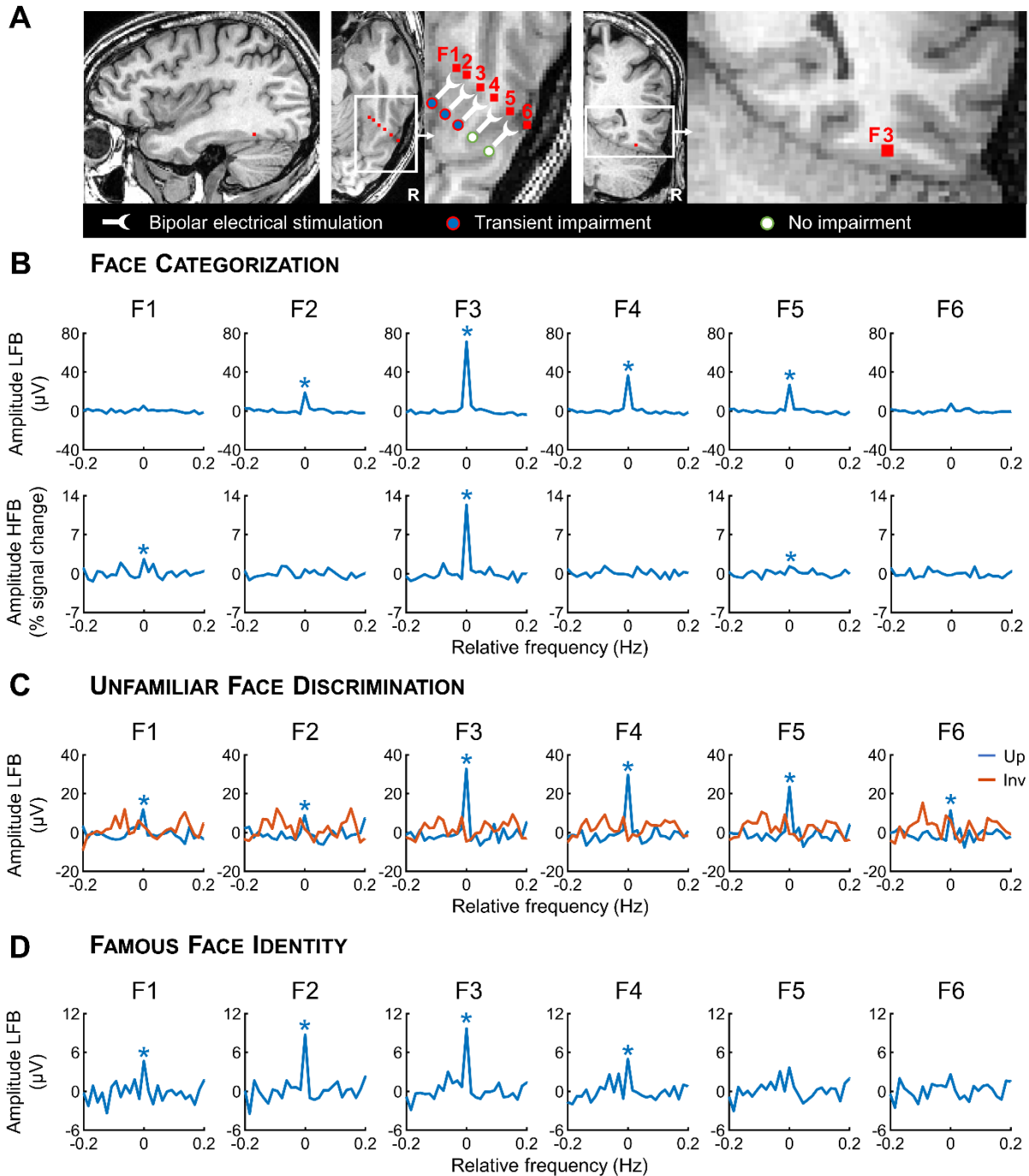


**Figure 3.** Anatomical and functional location of the stimulation sites inducing transient FIR impairment in CJ. **A.** Anatomical location of electrode F (in red) in sagittal, axial and coronal MRI slices. The electrode contact associated with the most consistent FIR impairment upon electrical stimulation was F3, located in the lateral portion of the middle fusiform gyrus (LatMidFG). **B.** Face-selective intracerebral responses recorded on electrode F (Face

*Categorization paradigm; Jonas et al., 2016) in the low-frequency bands (LFB, above) and high-frequency bands (HFB, below). These responses were quantified by first segmenting the baseline-corrected FFT spectrum into 12 segments centered at the face frequency and its harmonics up to 16.8 Hz (i.e., 1.2, 2.4, 3.6, etc., removing the base frequency and its harmonics at 6 and 12 Hz). The 12 segments were then summed. The 0 mark corresponds to the face frequency. C. Intracerebral responses to unfamiliar faces recorded on electrode F in the low-frequency bands for both upright and inverted faces (Unfamiliar Face Discrimination paradigm; Liu-Shuang et al., 2014; Jacques et al., 2020). These responses were quantified similarly as for the Face Categorization experiment above, except that 9 harmonics were summed. D. Intracerebral responses to upright famous faces recorded on electrode F in the low-frequency bands (Famous Face Identity paradigm; Zimmermann et al., 2019; 9 harmonics here). (\*) indicates significant responses at  $p < 0.001$ .*

In the famous face pointing task, CJ was asked to point to the famous face among 3 faces (**Figure 2A; Video S1**). When electrically stimulating contacts F1-F2, F2-F3 and F3-F4, she was transiently impaired at pointing to the famous face (**Figure 4**). Her performance was at ceiling outside stimulation but dropped significantly during stimulation time (on F1-F2: 100% accuracy outside stimulation [16/16 trials] vs. 66.67% [4/6] during stimulation;  $\chi(1) = 5.867$ ,  $p = 0.015$ ; on F2-F3: 100% accuracy outside stimulation [18/18 trials] vs. 16.67% [1/6] during stimulation;  $\chi(1) = 18.3947$ ,  $p < 0.001$ ; on F3-F4: 100% accuracy outside stimulation [18/18 trials] vs. 42.86% [3/7] during stimulation;  $\chi(1) = 12.245$ ,  $p < 0.001$ ). During these impaired stimulation sessions, CJ repeatedly stated that the faces looked the same (see **Video S1** for an example): “*they were the same three faces*”, “*they had all the same face*” (stimulation F1-F2, number 1); “*the two faces on the right side were the same*”, “*the face was smoother, as if his features was difficult to see*”, “*the facial features were more homogeneous, like a diagram*” (stimulation F1-F2, number 31); “*I did not see anyone I recognized*”, “*they all had the same face*”, “*I could not see one face different from the others*” (stimulation F2-F3, number 2); “*they were all the same, I did not see any difference between the three faces*”, “*they had all the same face*” (stimulation F2-F3, number 32); “*they were all the same*”, “*it was the same person*”, “*they all had the same face and it was a mix of the three*” (stimulation F3-F4, number 33); “*they were*



*all the same*", "they had all the same face" (stimulation F2-F3, number 32). For this last stimulation on F2-F3, she also reported seeing a slight physical distortion of the face: "they were all bearded, and one face was distorted: the eyes came out too much". By contrast, when stimulating more laterally in the right MTG (contacts F4-5 and F5-6), there were no famous face pointing impairments (**Figure 4; Table S2**).

After 5 stimulation sessions eliciting a FIR impairment, CJ was presented with the missed trials and asked to perform the task again. She readily pointed to the famous face identity, without errors (6/6 trials). These trials were not included in the analyses of performance (as reported in **Figure 4**). Also, immediately after each of these 5 stimulation sessions, she was asked to indicate verbally if these trials had been presented during the stimulation procedure. CJ was always able to remember the trials that were presented during the stimulation procedure (6/6, 100%) and correctly excluded the distractors (7/7, 100%).

In the face identity matching task, CJ had to match a target face with another photograph of the same identity, using either famous or unfamiliar faces (**Figure 2B; Videos S2 and S3**). For famous faces, upon electrical stimulation of contacts F2-F3 and F3-F4, CJ was unable to perform the task (no answer during stimulation, **Figure 4; Table S2**). CJ's performance dropped significantly during stimulation time (on F2-F3: 100% accuracy outside stimulation [12/12 trials] vs. 0% [0/5] during stimulation;  $\chi(1) = 17$ ,  $p < 0.001$ ; on F3-F4: 100% accuracy outside stimulation [9/9 trials] vs. 0% [0/4] during stimulation;  $\chi(1) = 13$ ,  $p < 0.001$ ). It appears that CJ was unable to respond because, as she repeatedly stated, the faces looked the same to her (see **Video S2** for an example): "I could not tell the difference between the two", "they were the same" (stimulation F2-F3, number 6); "they were all the same", "they were mixed" (stimulation F2-F3, number 36); "it was a mix of both, and both were identical" (stimulation F2-F3, number 7); "It was twice the same face but a mix of both", "as if they had a child together" (stimulation F3-F4, number 37). For one stimulation session, she also hinted at slight changes of the face percept: "they all looked alike but they were weird", "they looked aggressive and very much alike" (stimulation F2-F3, number 6). Stimulations performed outside of these two

critical sites (i.e., on F1-F2, F4-F5, F5-F6) did not elicit any famous face identity matching impairment (**Figure 4; Table S2**). However, note that for one stimulation session on F1-F2 in the right LatMidFG (number 5), CJ hesitated for two trials during stimulation but finally pointed out the correct faces. After stimulation, she stated: *“all three were the same”, “I saw the three same faces”*.

Electrical stimulation of the same contacts F2-F3 and F3-F4 also elicited transient deficit at matching unfamiliar faces (**Figure 4; Table S2**). CJ's performance dropped significantly during stimulation (on F2-F3: 100% accuracy outside stimulation [9/9 trials] vs. 0% [0/4] during stimulation;  $\chi(1) = 13$ ,  $p < 0.001$ ; on F3-F4: 100% accuracy outside stimulation [10/10 trials] vs. 50% [2/4] during stimulation;  $\chi(1) = 5.833$ ,  $p = 0.016$ ). As in previous stimulation sessions, she repeatedly stated that the faces looked the same (see **Video S3** for an example): *“everyone was the same”, “I didn't see any difference between the three faces”, “the faces were coherent but similar”* (stimulation F3-F4, number 40); *“they were the same women”* (stimulation F2-F3, number 39). For this last stimulation on F2-F3, she also reported a face distortion: *“they were all the same, had huge teeth and were scary”*. Stimulation sessions outside of these two critical sites did not elicit unfamiliar face identity matching impairment (on F1-F2 or F4-5; **Figure 4; Table S2**).

Finally, we also asked CJ to perform a famous face naming task when stimulating electrode F. CJ failed only on one trial during stimulation of F2-F3 (no answer, with no visual perceptual change, **Figure 4; Table S2**). As a result, there was no statistical difference between her performance at naming faces outside and during stimulation (on F2-F3: 100% accuracy outside stimulation [5/5 trials] vs. 75% [3/4] during stimulation;  $\chi(1) = 1.406$ ,  $p = 0.236$ ). However, since we observed that CJ sometimes hesitated before giving the correct name during stimulation, we measured her response times (RTs) for F1-F2, F2-F3 and F3-F4 stimulations. Across these three stimulation sites, her mean RTs were twice higher during stimulation (mean RTs across 5 trials:  $1574 \pm 1072$  ms) than outside stimulation (mean RTs across 12 trials:  $786\text{ms} \pm 223$ ). However, due to the small number of trials, this difference was

only marginally significant ( $t(15) = 1.630$ ,  $p = 0.088$ ; one-sided independent samples t-test with unequal variance). Moreover, for two trials during stimulation of F2-F3 and F3-F4 (1 trial each), CJ reported a substantial change of face percept that did not prevent her to state the correct name. She stated: "*it was like there was another face, like if it wasn't him on the other side of the face*", "*this side (the left), it was not him*", "*his eye wasn't his eye*", "*it was not shifted, it was tidy*" (stimulation F2-F3, number 21); "*it seems like it is not his face*", "*it was a coherent face, but the eyes were not the same*", "*it was the same face but without wrinkles, smoother*" (stimulation F3-F4, number 22). Stimulations of other F contacts did not evoke facial visual changes.

### **3.3 Stimulating the right lateral fusiform gyrus induces the visual illusion that all faces look the same**

As indicated above, along with the objective behavioral impairment observed during stimulation of the right LatMidFG (stimulations of F1-F2, F2-F3 and F3-F4), CJ reported at least two types of subjective visual changes. The most frequent was an illusion that all faces looked the same (occurring in 14 out of 22 stimulation sessions performed with tasks involving several faces simultaneously, i.e., pointing and matching tasks, with 13 out of these 14 stimulations eliciting at least one error during stimulation). Most of the time, CJ stated that she simply could not tell the differences between faces, but sometimes reported that faces looked alike because they were mixed. Occasionally, CJ also reported perceptual changes of a different nature (change of the face into another face, replacement of face parts, scary or aggressive expressions, for 5 out the 27 stimulation sessions with faces, irrespective of the task, with 3 out of these 5 stimulations eliciting at least one error during stimulation). With one slight exception perhaps (one trial during stimulation on F2-F3 with the famous face pointing task; *one face was distorted, the eyes came out too much*), there was no change in the perception of the spatial configuration of the face(s). These two types of visual phenomena (faces looking the same and perceptual changes) were both reported during the same stimulation session on three occasions. When these two phenomena co-occurred, it was

always during tasks involving several faces (i.e., pointing or matching). Illusions that all faces looked the same were more frequently reported than other facial changes (14/22 stimulations sessions of the right LatMidFG, 63.6%, versus 5/27, 18.5%;  $\chi(1) = 10.395$ ,  $p = 0.001$ ).

### **3.4 Stimulating the right lateral fusiform gyrus does not impair non-face tasks**

We also tested stimulation of electrode F contacts during two non-face tasks: a famous name pointing task and a famous building naming task. Stimulating contacts F1-F2, F2-F3, F3-F4 and F4-F5 did not evoke any impairment at naming famous buildings (**Figure 4; Table S2**). CJ immediately named all the buildings (100% of accuracy outside and during stimulation for each site, **Figure 4**) and, unlike for the face naming task above, did not report any change of percept nor show hesitation. For the famous name pointing task (**Figure 2A**), CJ performed correctly all trials, no matter the stimulation site and time period (**Figure 4; Table S2**), without reporting any visual perceptual changes.

### **3.5 Face-selectivity of the critical stimulation sites**

The fMRI face localizer experiment revealed eight face-selective clusters in CJ's occipito-temporal cortex with a threshold of  $p < 0.001$  ( $z$ -score  $> 3.09$ , uncorrected) and a minimum cluster size of 10 contiguous  $2.5 \times 2.5 \times 2.5$  mm<sup>3</sup> voxels. The clusters were located bilaterally in the LatMidFG, lateral occipital complex (including the inferior occipital gyrus and lateral occipital cortex), and superior temporal sulcus (**Figure 6A**). In total, there were 212 significant voxels activated in the right hemisphere and 160 voxels in the left hemisphere. The largest cluster was located in the right LatMidFG, with 115 contiguous voxels above threshold. The Talairach coordinates of the peak SNR voxel (i.e.,  $x = 38$ ,  $y = -61$ ,  $z = -12$ ) in the right LatMidFG cluster were consistent with previous studies localizing it as the FFA ([Kanwisher et al. 1997](#); [Gao et al. 2018, 2019](#)). Electrode F crossed this right LatMidFG cluster (**Figure 6A**). To examine the face-selective responses in each F contact, we created masks with a 1 mm radius from the center coordinates of each contact (see **Supplementary Information; Figure 6B**).

The fMRI face-selective activations overlapped well with multiple contacts of electrode F, including critical contacts F1, F3 (highest SNR) and F4.

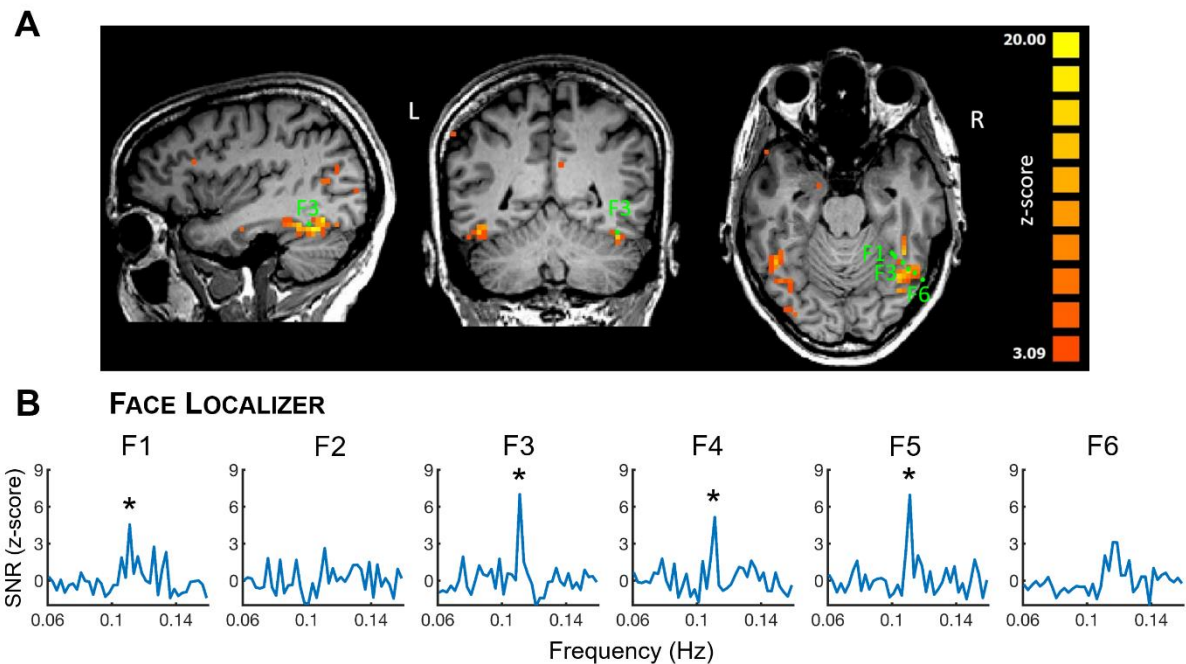


**Figure 6. A.** fMRI face-localizer using the Fast Periodic Stimulation approach (Gao et al. 2018; threshold of  $p < 0.001$ ,  $z\text{-score} > 3.09$ , uncorrected) with electrode F electrode superimposed (in green). Here coordinates on the z-axis of the whole electrode F are those of contact F3 for all contacts to be displayed on the same axial slice. **B.** Frequency spectra of electrode F contacts (mask with 1 mm radius). Asterisks indicate significant face-selective response ( $z\text{-score} > 3.09$ ).

In SEEG with FPVS paradigms, significant face-selective responses ( $p < 0.001$ ) occurring exactly at 1.2 Hz and harmonics were found on contacts F2 to F5 in the low-frequency bands (Figure 5B). Impressively, among all the 147 of intracerebral contacts implanted in subject CJ, the largest face-selective response amplitude was found on contact F3 in the right LatMidFG (Figure 7A). Other face-selective responses were found on contacts in the right and left ATL (8 contacts in each ATL region; see Figure 7A). Face-selective responses in HFB were found on contacts F1, F3 and F5, with the largest response - by far - also observed on F3 among all the 147 intracerebral contacts implanted in subject CJ (Figure 5B). Significant responses in HFB were also found in left and right ATL (1 contact each). In

sum, the largest face-selective responses, both for low- and high-frequency bands, were found on contact F3, that is the most critical contact during DES (**Figure 4**).

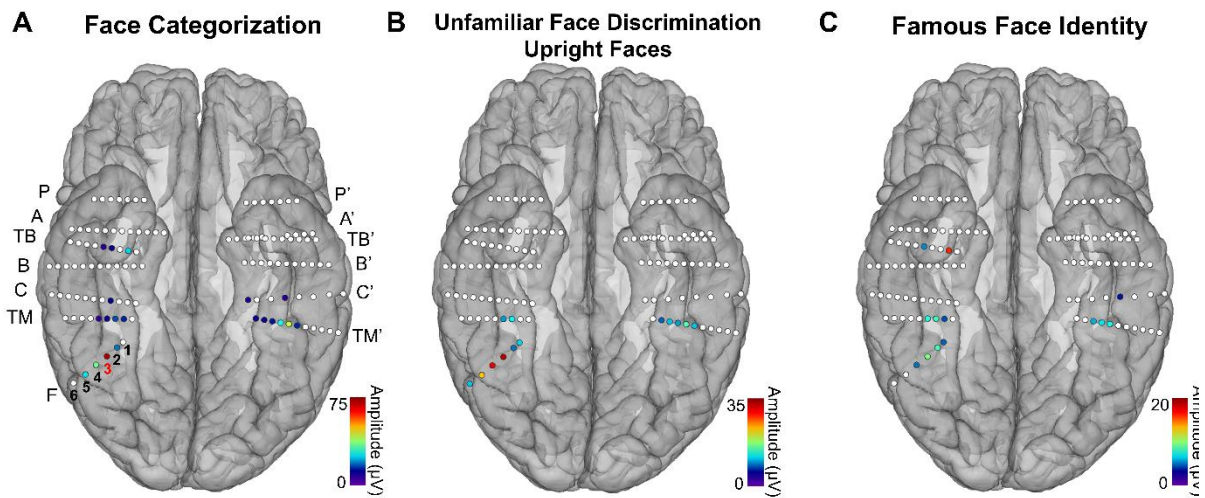


**Figure 7.** Spatial distribution of intracerebral contacts in CJ's VOTC and significant responses to three FPVS paradigms. **A.** Amplitudes of significant face-selective responses are plotted for the Face Categorization paradigm. **B.** Amplitudes of significant unfamiliar face discrimination responses. **C.** Amplitudes of significant famous face identity responses. Intracerebral contacts located in the VOTC are plotted in the native MRI space of CJ's brain using a reconstructed cortical surface. Each circle represents a single intracerebral contact; white circles depict contacts with no significant response while colored circles indicate significant contacts and their respective baseline-corrected amplitude. Each electrode's name is displayed on its outer side and contacts are numerically labelled, i.e., F1 is the most medial contact of electrode F and F6 is its most lateral contact. Contact F3 eliciting the strongest FPVS responses and the most reproducible electrical stimulation effects is highlighted in red.

### 3.6 Are the stimulation sites located in a region sensitive to face identity?

Unfamiliar face discrimination responses in the low-frequency bands were found in the upright condition on contacts F1, F2, F3, F4, F5 and F6 (**Figure 5C**), as well as on 2 contacts in the right ATL and 5 in the left (**Figure 7B**). Among all contacts implanted in subject CJ, the largest response amplitude was again found on contact F3. These responses were specific to upright faces, as no significant responses were found in the inverted condition on the very same contacts (**Figure 5C**). Subtracting responses in the inverted condition from responses in

the upright condition showed a strong and significant inversion effect on contacts F3, F4 and F5, as well as on one contact in the left ATL. Again, the largest (difference) amplitude (between upright and inverted faces) was found on contact F3.

In the Famous Face Identity paradigm, significant responses were recorded on contacts F1, F2, F3 and F4 (**Figure 5D**), as well as on 5 contacts in the right ATL and 4 in the left. Among all F contacts, the largest response amplitude was again found on contact F3, which was the second largest amplitude among all implanted contacts overall (**Figure 7C**).

Altogether, these results show that the stimulation sites evoking transient face identity recognition deficits (F1, F2, F3, F4) were located in a region sensitive to individual face identity. Moreover, and impressively, the electrode contact evoking transient FIR deficits with the highest reproducibility (F3) also recorded the largest face-selective amplitude, and the largest or second largest amplitude in the Unfamiliar Face Discrimination and Famous Face Identity paradigms, respectively.

#### **4. DISCUSSION**

For the first time to our knowledge, we show that DES to a face-selective region of the right LatMidFG in the human brain – a region usually dubbed the FFA – transiently impairs FIR. This objective behavioral effect almost systematically occurs when the patient subjectively perceives the simultaneously presented face pictures as being of the same identity. It is limited to a few contiguous electrode contacts in this region and is highly reproducible across a variety of tasks and stimuli (mostly nonverbal tasks such as pointing and matching for both familiar and unfamiliar face identities). Although clinical constraints prevented the testing of a wide range of non-face material (e.g., matching of similar visual object shapes for instance), the effect appears limited to faces, with preserved recognition of other visual entities (buildings, written names) upon stimulation (and no reported change of percept). Importantly, there is a striking correspondence between the location of the most critical DES contact and the peak of both fMRI and electrophysiological face-selectivity, as well as neural sensitivity to unfamiliar

and familiar face identity recognition. In summary, beyond lesion studies, and beyond numerous neuroimaging and intracranial electrophysiological studies that have singled out the contribution of this hominoid-specific region of the VOTC in dealing selectively with face stimuli, the present observations provide arguably the first direct evidence for the critical role of the right FFA in human FIR.

#### **4.1 The right lateral middle FG is critical for face identity recognition**

Neuroimaging (fMRI) studies, mainly relying on adaptation/repetition suppression paradigms, have shown that the FFA is involved in differentiating between face identities (e.g., [Gauthier et al. 2000](#); [Schiltz and Rossion 2006](#); [Gilaie-Dotan et al. 2010](#); [Ewbank et al. 2013](#); [Hermann et al. 2017](#))<sup>1</sup>. These fMRI studies have often showed the strongest adaptation effects in this region, both for familiar and unfamiliar faces (e.g., [Hermann et al. 2017](#)), albeit with little evidence of a stronger effect in the right hemisphere (e.g., [Davies-Thompson et al. 2013](#)), and an exploration often limited to pre-defined face-selective regions of interest. A recent large-scale intracerebral recording study with a frequency-tagging adaptation paradigm (as also used here) also showed the largest effect for discriminating pictures of unfamiliar faces in the right LatMidFG ([Jacques et al. 2020](#)).

While these studies point to a clear contribution of the right FFA in FIR, i.e., beyond its sensitivity to faces as a category, its causal role has remained, surprisingly, unproven. Indeed, as mentioned in the introduction, lesion studies of cases of prosopagnosia or FIR impairments

---

<sup>1</sup> Studies using multivariate pattern analyses (MVPA) across voxels, without adaptation, have sometimes also successfully decoded different identities in this region (e.g., [Nestor et al. 2011](#); [Goesaert and Op de Beeck 2013](#); [Tsantani et al. 2021](#)). However, there is no reason to expect that different face identities should be discriminable reliably at the voxel resolution (containing millions of neurons in the human fusiform gyrus; see [Chance et al. 2013](#)). Hence, these effects are generally weak, inconsistent across studies and likely to merely reflect image-based differences (see the critical view of [Rossion 2014](#)).



often but not always involve this region (see for instance the extensively documented case of prosopagnosia PS initially reported in [Rossion et al. 2003](#), with a structurally intact right LatMidFG and normal level of face-selectivity in this region; [Rossion 2022](#); see also [Bouvier and Engel 2006](#); [Cohen et al. 2019](#)). In this context, it is important to stress that DES, one of the most efficient approaches to identify critical regions for cognitive functions, had not demonstrated causal involvement of the (right) LatMidFG in FIR before the present case. Previous DES studies with subdural electrodes (electrocorticography or ECoG) mostly reported subjective face perceptual changes (“face distortions”) without (behavioral) evidence of FIR deficits ([Parvizi et al. 2012](#); [Rangarajan et al. 2014](#); [Schalk et al. 2017](#); [Schrouff et al. 2020](#); [Sanada et al. 2021](#)). While our research group has been performing DES in the human VOTC of implanted patients for more than a decade, prior to the present case, rare cases of objective FIR impairment (i.e., drop in FIR performance) have been observed during DES to other face-selective regions in the right hemisphere: the IOG (i.e., OFA; subject KV: [Jonas et al. 2012, 2014](#)) and the anterior portion of the fusiform gyrus (i.e., AntFG; subject CD: [Jonas et al. 2015](#); subject DN: [Volfart et al. 2022](#); for review see [Jonas and Rossion 2021](#)). Yet, in another case study (MB; [Jonas et al. 2018](#)), DES to the right FFA as performed here in CJ elicited subjective visual changes corresponding to face *palinopsia*, the patient perceiving features of a previously seen face superimposed on the currently presented face identity. This may be similar to some of the visual changes reported by the present case CJ, especially when the latter was presented with only one face at a time (i.e., during the face naming task; e.g., “*his eye wasn’t his eye*”). However, as in other cases of DES to the right FFA reported mainly by Parvizi and colleagues ([Parvizi et al. 2012](#); [Rangarajan et al. 2014](#)), there was no evidence of a FIR impairment provided in this previous case ([Jonas et al. 2018](#)).

The current case report therefore goes well beyond previous studies by showing, through an objective behavioral evaluation of performance during and outside stimulation, a critical role of the right face-selective LatMidFG, or right FFA, in FIR. Importantly, as shown also for the recently reported case DN stimulated in the AntFG ([Volfart et al. 2022](#)), most of the tasks used,

in fact those that led to the clearest deficits, did not require verbal output (famous face pointing task, famous face matching task, unfamiliar face matching task), ensuring that the transient impairment in FIR was not due to a deficit at accessing names (as it might have been in several early ECoG DES studies, often performed over the left LatMidFG; [Allison et al. 1994](#); [Puce et al. 1999](#)).

#### **4.2 What is the role of the right LatMidFG in face identity recognition?**

The present case study of CJ provides evidence that the face-selective right LatMidFG plays a critical role in the ability to pick out the idiosyncratic visual cues that makes every face unique, regardless of whether this face identity has been previously encoded or not in memory. This claim rests on several elements. First, stimulating the right LatMidFG elicited a transient inability to match the identity of faces presented simultaneously, using famous and, more importantly, unfamiliar faces. Second, when stimulating the same sites, CJ was able to point out famous names among unfamiliar ones, excluding a general disruption of semantic memory or person recognition. Third, among all implanted contacts, those evoking the transient FIR impairment recorded the largest FPVS unfamiliar face discrimination responses (as also found at the group level; [Jacques et al. 2020](#)). Fourth, whenever she was transiently impaired at performing the FIR task, subject CJ consistently (i.e., 13 out of 14 stimulation sessions) reported the visual illusion that “*all faces looked the same*”. We hypothesize that the loss of the behavioral ability to discriminate different faces identities resulted from this perception that all faces look the same. This subjective report is similar to a patient with an undefined lesion in the right LatMidFG describing an inability to distinguish between faces as part of her epileptic aura, this aura being reproduced by electrically stimulating with subdural electrodes over the right LatMidFG brain lesion ([Mundel et al. 2003](#)).

As noted above, this view of the right LatMidFG as playing a critical role in individuating faces is supported by fMRI studies showing adaptation effects with pictures of unfamiliar faces (e.g., [Gauthier et al. 2000](#); [Gilaie-Dotan et al. 2010](#); [Ewbank et al. 2013](#); [Hermann et al. 2017](#); [Kovács 2020](#)), intracerebral recordings showing the largest FPVS unfamiliar face

discrimination responses in the right LatMidFG among all VOTC regions (Jacques et al. 2020), as well as studies showing a lack of such adaptation effects in this region in cases of prosopagnosia (Schiltz et al. 2006; Dricot et al. 2008; see also Steeves et al. 2009). Further neuroimaging studies have provided evidence that this region is specifically involved in holistic/configural representation of face identity (i.e., face identities being represented as integrated wholes rather than as a collection of independent features; e.g., Yovel and Kanwisher 2005; Mazard et al. 2006; Schiltz and Rossion 2006; Andrews et al. 2010; Schiltz et al. 2010; Zhang et al. 2012; Zhou et al. 2018).

Whether or not the face-selective region of the LatMidFG differentially processes unfamiliar and familiar faces is highly debated (Gobbini and Haxby 2007; Natu and O'Toole 2011). Neuroimaging studies have found differential responses between familiar and unfamiliar faces in the LatMidFG (Sergent et al. 1992; Rossion, Schiltz, et al. 2003; Natu and O'Toole 2015) but these effects are inconsistent (i.e., relative increases or decreases to familiar faces) and other studies did not find any difference (e.g., Leveroni et al. 2000; Ramon et al. 2015). Here, using a FPVS famous face identity paradigm in electrophysiology, we recorded large famous/unfamiliar discrimination responses in the right LatMidFG (and in the right ATL) (Figures 5 and 7). These results suggest that the right LatMidFG is sensitive to the familiarity status of the faces, although whether these responses reflect local processes or reentrant neural activity from more anterior regions involved in semantics is undetermined (but see Quiroga et al. in press).

During DES to the critical contacts, beyond the frequent perception that all faces looked the same (63.6% of the stimulations), CJ also more rarely (18.5%) reported various changes of the face percept such as a partial change of the face into another face (*“it was like there was another face, like if it wasn't him on the other side of the face”*), changes of face parts (*“his eye wasn't his eye”*), scary or aggressive expressions (*“they looked aggressive”*) and, for one stimulation only, a slight change of the facial configuration (*“the eyes came out too much”*). Such perceptual changes, which have been defined as 'metamorphopsia' and linked to the

right LatMidFG even before its definition as a key face-selective region (Seron et al. 1995), are more similar to the most frequent visual changes reported by DES applied to this region with ECoG (Parvizi et al., 2012; Rangarajan et al., 2014; Schalk et al., 2017; Schrouff et al., 2020; Sanada et al., 2021). However, as indicated above, metamorphopsia, or face palinopsia, in isolation, do not provide evidence for a critical role of the LatMidFG in FIR, for several reasons. First, there was no report of such phenomena for most of the stimulations disrupting FIR in CJ. Second, DES inside the right AntFG can impair FIR without any perceived distortion or even a change of percept at all (Jonas et al. 2015; Volfart et al. 2022). Third, such changes of the perceived face configuration do not prevent recognizing the identity of faces (Parvizi et al. 2012), as also found in subject MB with palinopsia (Jonas et al. 2018). As a matter of fact, even the present case was able to recognize the identity of faces in most of the trials of the face naming task, albeit with a substantial response delay. Finally, cases of prosopagnosia do not usually report facial changes along with their FIR impairment (but see Hécaen and Angelergues 1962).

In summary, while the reasons why DES to the (face-selective) right LatMidFG often evokes spectacular perceptual changes described as metamorphopsia (Parvizi et al. 2012) or face palinopsia (Jonas et al. 2018) – remain unknown, these phenomena cannot be systematically and unambiguously related to FIR. In contrast, the consistent report of subject CJ that *'all faces look the same'*, certainly probed by the concurrent presentation of several faces in our behavioral tasks (see also Jonas et al. 2014), is in line with her behavioral impairment at these tasks and a bulk of evidence supporting a role of this region in differentiating face identities regardless of their long-term familiarity status.

#### **4.3. A cortical network view of DES-related face identity recognition impairments**

It is important to stress that the right LatMidFG is not the only critical region supporting FIR, a function that, in humans, relies on a specialized right lateralized network of face-selective regions across the VOTC. Indeed, beyond evidence from lesion studies (Meadows 1974; Damasio et al. 1982; Sergent and Signoret 1992; Bouvier and Engel 2006; Sorger et al.

2007; Tranel et al. 2009; Cohen et al. 2019), transient inability to match the identity of unfamiliar faces has also been reported during DES of the right face-selective IOG/OFA and the right face-selective AntFG, located respectively posteriorly and anteriorly to the LatMidFG along the VOTC (Jonas et al. 2014; Volfart et al. 2022, respectively). Importantly, the critical contacts in these two regions recorded large frequency-tagged unfamiliar face discrimination responses, as in the present case report. As mentioned above, a large-scale mapping of FPVS unfamiliar face discrimination responses with SEEG showed that the highest proportion and the largest amplitude of responses were found along a strip of cortex including the right LatMidFG but also the IOG and AntFG, with the largest amplitude recorded in the LatMidFG (Jacques et al. 2020). As for fMRI adaptation effects for unfamiliar faces, they are also found in the IOG (Gauthier et al. 2000; Eger et al. 2004; Schiltz and Rossion 2006; Gilaie-Dotan et al. 2010; Ewbank et al. 2013; Hermann et al. 2017; Hughes et al. 2019; Rostalski et al. 2020), and the lack of evidence for effects anterior to the LatMidFG is likely to be due to severe magnetic susceptibility artifacts affecting the ventral ATL (Wandell 2011; Rossion et al. 2018; Volfart et al. 2022).

Given that the FIR function appears to be distributed across several face-selective VOTC regions, the behavioral impairment of the present case CJ may be due to transient disruption of several regions connected to the stimulated site beyond the right FFA. That is, the right LatMidFG should be seen as a key node of the cortical face network, with other nodes (ipsilaterally or even in the other hemisphere), or even the entire network supporting FIR, affected through current spread along tract connections (Tolias et al. 2005; Moeller et al. 2008; Mandonnet et al. 2010; Borchers et al. 2012; Rolston and Chang 2018; Perrone-Bertolotti et al. 2020; Jonas and Rossion 2023). Consistent with this view, it has been shown that DES of the LatMidFG (behaviorally affecting face detection) spreads anteriorly and posteriorly across the VOTC and predominantly to face-selective sites (Keller et al. 2017).

### **4.3 Why are FIR impairments following DES so rarely observed?**

Even though the cortical network supporting FIR is widely distributed across the VOTC (Jacques et al. 2020) and DES has been increasingly used during the last decade to

understand this function (for review see [Jonas and Rossion 2023](#)), very few DES studies so far have reported objective FIR impairments ([Jonas et al. 2012, 2014, 2015](#); [Volfart et al. 2022](#); the present study). Why are such observations so rare?

Here, we argue that inducing a FIR impairment by DES requires a number of conditions that are unlikely to happen in a clinical context. First, as mentioned above, behavioral tasks specifically designed to test this function are required, ideally, without verbal output to avoid potential confound with naming and with a sufficient number of simulations to provide quantitative measurements of the DES effects in terms of accuracy and response time ([Jonas et al. 2014](#); [Volfart et al. 2022](#); see also [Chong et al. 2013](#); [Keller et al. 2017](#) for face detection tasks). In contrast, most of the ECoG DES studies over the LatMidFG only required subjects to view a human face at bedside, and to report whether the face remained the same or was distorted ([Rangarajan et al. 2014](#); [Schalk et al. 2017](#); [Schrouff et al. 2020](#); [Sanada et al. 2021](#); see also [Jonas et al. 2018](#) in SEEG). Moreover, unless response times are systematically measured in a large number of trials, a famous face naming task (in which face identities are presented one at a time) may not be well-suited to elicit FIR impairment during right LatMidFG stimulation ([Parvizi et al. 2012](#); [Jonas et al. 2018](#); the present case). Instead, forced-choice recognition or matching tasks with several faces presented simultaneously as in the present case may be required to elicit these FIR impairments during stimulation. Second, while ECoG DES probably disrupts a relatively large cortical zone, explaining global distortions of the faces, sometimes even when stimulating non-face-selective sites ([Parvizi et al. 2012](#); [Rangarajan et al. 2014](#); [Schrouff et al. 2020](#)), SEEG, thanks to intracortical DES, may be better suited to more specifically disturb the function of local populations of neurons critically involved in FIR. Third, the DES electrode should be located specifically (by chance) in one of the most face-selective regions of the VOTC. However, the precise localization and number of face-selective clusters, especially within the LatMidFG, vary considerably across individual brains and, besides a major distinction between medial and lateral fusiform gyri ([Weiner and Grill-Spector 2012](#); [Weiner et al. 2014](#)), is not well predicted by the individual anatomy ([Rossion et al. 2012](#); [Zhen](#)

et al. 2015; Gao et al. 2022). Here, for instance, the critical contacts were not only located in a face-selective region of the right LatMidFG: they fell into the largest face-selective cluster as identified in fMRI (**Figure 6A**) and, most importantly, were associated with the largest face-selectivity and face identity electrophysiological indexes as obtained with frequency-tagging (**Figure 7**). This is unlikely to occur in most clinical investigations of the VOTC for intractable epilepsy. While these factors are likely to explain the rarity of stimulation-induced FIR impairments, other interindividual variables (e.g., level of connectivity with other nodes of the network of the stimulated site, stimulation parameters, electrode orientation with respect to the cortex, relative distance to grey and white matters, performance at FIR outside stimulation, etc.) may influence whether DES over the right FFA of a given individual will or will not elicit a transient FIR impairment, and future research will be needed to clarify this issue.

## 5. ACKNOWLEDGEMENTS

We thank subject CJ for her involvement and willingness to participate in the study. We thank Dr. H el ene Brissart for performing CJ's neuropsychological assessment, and Justine David for her help in collecting stimulation data. This work was supported by the Excellence of Science (EOS) program (HUMVISCAT30991544) and an ERC ADG HUMANFACE 101055175 to BR. AV was supported by the University of Lorraine (MESRI doctoral grant) and by a postdoctoral grant from the University of Louvain.

## 6. REFERENCES

- Allison T, Ginter H, McCarthy G, Nobre AC, Puce A, Luby M, Spencer DD. 1994. Face recognition in human extrastriate cortex. *J Neurophysiol.* 71:821–825.
- Andrews TJ, Davies-Thompson J, Kingstone A, Young AW. 2010. Internal and external features of the face are represented holistically in face-selective regions of visual cortex. *J Neurosci.* 30:3544–3552.
- Aron O, Jonas J, Colnat-Coulbois S, Maillard L. 2021. Language mapping using stereo electroencephalography: a review and expert opinion. *Front Hum Neurosci.* 15:619521.
- Barton JJS. 2008. Structure and function in acquired prosopagnosia: Lessons from a series of 10 patients with brain damage. *J Neuropsychol.* 2:197–225.
- Benedict RH. 1997. Brief visual memory test–revised: Professional manual. Odessa, FL: Psychological Assessment Resources.

- Benton AL, Sivan AB, Hamsher K, Varney NR, Spreen O. 1983. Benton facial recognition: Stimulus and multiple choice pictures. Psychological Assessment Resources Inc. ed. Lutz, FL.
- Borchers S, Himmelbach M, Logothetis N, Karnath H-O. 2012. Direct electrical stimulation of human cortex — the gold standard for mapping brain functions? *Nat Rev Neurosci.* 13:63–70.
- Bouvier SE, Engel SA. 2006. Behavioral deficits and cortical damage loci in cerebral achromatopsia. *Cereb Cortex.* 16:183–191.
- Bryant KL, Preuss TM. 2018. A comparative perspective on the human temporal lobe. In: Bruner E., Ogihara N., Tanabe HC, editors. *Digital Endocasts: From Skulls to Brains. Replacement of Neanderthals by Modern Humans Series.* Tokyo: Springer Japan. p. 239–258.
- Buschke H. 1973. Selective reminding for analysis of memory and learning. *J Verbal Learn Verbal Behav.* 12:543–550.
- Busigny T, Rossion B. 2010. Acquired prosopagnosia abolishes the face inversion effect. *Cortex.* 46:965–981.
- Chance SA, Sawyer EK, Clover LM, Wicinski B, Hof PR, Crow TJ. 2013. Hemispheric asymmetry in the fusiform gyrus distinguishes *Homo sapiens* from chimpanzees. *Brain Struct Funct.* 218:1391–1405.
- Chen X, Liu X, Parker BJ, Zhen Z, Weiner KS. 2022. Functionally and structurally distinct fusiform face area(s) in over 1000 participants.
- Chong SC, Jo S, Park KM, Joo EY, Lee M-J, Hong SC, Hong SB. 2013. Interaction between the electrical stimulation of a face-selective area and the perception of face stimuli. *NeuroImage.* 77:70–76.
- Cohen AL, Soussand L, Corrow SL, Martinaud O, Barton JJS, Fox MD. 2019. Looking beyond the face area: lesion network mapping of prosopagnosia. *Brain.* 142:3975–3990.
- Crawford JR, Howell DC. 1998. Comparing an individual's test score against norms derived from small samples. *Clin Neuropsychol.* 12:482–486.
- Damasio AR, Damasio H, Van Hoesen GW. 1982. Prosopagnosia: anatomic basis and behavioral mechanisms. *Neurology.* 32:331–341.
- Davies-Thompson J, Newling K, Andrews TJ. 2013. Image-invariant responses in face-selective regions do not explain the perceptual advantage for familiar face recognition. *Cereb Cortex N Y NY.* 23:370–377.
- Deloche G, Hannequin D. 1997. Test de dénomination orale d'images: DO 80. Éd. du Centre de psychologie appliquée.
- Dricot L, Sorger B, Schiltz C, Goebel R, Rossion B. 2008. The roles of “face” and “non-face” areas during individual face perception: evidence by fMRI adaptation in a brain-damaged prosopagnosic patient. *NeuroImage.* 40:318–332.
- Eger E, Schyns PG, Kleinschmidt A. 2004. Scale invariant adaptation in fusiform face-responsive regions. *NeuroImage.* 22:232–242.
- Ewbank MP, Henson RN, Rowe JB, Stoyanova RS, Calder AJ. 2013. Different neural mechanisms within occipitotemporal cortex underlie repetition suppression across same and different-size faces. *Cereb Cortex.* 23:1073–1084.
- Gao X, Gentile F, Rossion B. 2018. Fast periodic stimulation (FPS): a highly effective approach in fMRI brain mapping. *Brain Struct Funct.*



- Gao X, Vuong QC, Rossion B. 2019. The cortical face network of the prosopagnosic patient PS with fast periodic stimulation in fMRI. *Cortex*. 119:528–542.
- Gao X, Wen M, Sun M, Rossion B. 2022. A genuine interindividual variability in number and anatomical localization of face-selective regions in the human brain. *Cereb Cortex*. bhab519.
- Gauthier I, Tarr MJ, Moylan J, Skudlarski P, Gore JC, Anderson AW. 2000. The fusiform “face area” is part of a network that processes faces at the individual level. *J Cogn Neurosci*. 12:495–504.
- Gilaie-Dotan S, Gelbard-Sagiv H, Malach R. 2010. Perceptual shape sensitivity to upright and inverted faces is reflected in neuronal adaptation. *NeuroImage*. 50:383–395.
- Gobbini MI, Haxby JV. 2007. Neural systems for recognition of familiar faces. *Neuropsychologia*. 45:32–41.
- Goesaert E, Op de Beeck HP. 2013. Representations of facial identity information in the ventral visual stream investigated with multivoxel pattern analyses. *J Neurosci*. 33:8549–8558.
- Grande KM, Ihnen SKZ, Arya R. 2020. Electrical stimulation mapping of brain function: a comparison of subdural electrodes and stereo-EEG. *Front Hum Neurosci*. 14:611291.
- Grill-Spector K, Weiner KS, Kay K, Gomez J. 2017. The functional neuroanatomy of human face perception. *Annu Rev Vis Sci*. 3:167–196.
- Hagen S, Jacques C, Maillard LG, Colnat-Coulbois S, Rossion B, Jonas J. 2020. Spatially dissociated intracerebral maps for face- and house-selective activity in the human ventral occipito-temporal cortex. *Cereb Cortex*. 30:4026–4043.
- Hécaen H, Angelergues R. 1962. Agnosia for faces (prosopagnosia). *Arch Neurol*. 7:92–100.
- Hermann P, Grotheer M, Kovács G, Vidnyánszky Z. 2017. The relationship between repetition suppression and face perception. *Brain Imaging Behav*. 11:1018–1028.
- Hermes D, Miller KJ, Vansteensel MJ, Aarnoutse EJ, Leijten FSS, Ramsey NF. 2012. Neurophysiologic correlates of fMRI in human motor cortex. *Hum Brain Mapp*. 33:1689–1699.
- Hughes BL, Camp NP, Gomez J, Natu VS, Grill-Spector K, Eberhardt JL. 2019. Neural adaptation to faces reveals racial outgroup homogeneity effects in early perception. *Proc Natl Acad Sci*. 116:14532–14537.
- Isnard J, Taussig D, Bartolomei F, Bourdillon P, Catenoix H, Chassoux F, Chipaux M, Clémenceau S, Colnat-Coulbois S, Denuelle M, Derrey S, Devaux B, Dorfmüller G, Gilard V, Guenot M, Job-Chapron A-S, Landré E, Lebas A, Maillard L, McGonigal A, Minotti L, Montavont A, Navarro V, Nica A, Reyns N, Scholly J, Sol J-C, Szurhaj W, Trebuchon A, Tyvaert L, Valenti-Hirsch MP, Valton L, Vignal J-P, Sauleau P. 2018. French guidelines on stereoelectroencephalography (SEEG). *Neurophysiol Clin, French Guidelines on Stereoelectroencephalography (SEEG)*. 48:5–13.
- Jacques C, Jonas J, Colnat-Coulbois S, Maillard L, Rossion B. 2022. Low and high frequency intracranial neural signals match in the human associative cortex. *eLife*. 11:e76544.
- Jacques C, Rossion B, Volfart A, Brissart H, Colnat-Coulbois S, Maillard LG, Jonas J. 2020. The neural basis of rapid unfamiliar face individuation with human intracerebral recordings. *Neuroimage*. 221:117174.
- Jonas J, Brissart H, Hossu G, Colnat-Coulbois S, Vignal J-P, Rossion B, Maillard L. 2018. A face identity hallucination (palinopsia) generated by intracerebral stimulation of the face-selective right lateral fusiform cortex. *Cortex*. 99:296–310.

- Jonas J, Descoins M, Koessler L, Colnat-Coulbois S, Sauvée M, Guye M, Vignal J-P, Vespignani H, Rossion B, Maillard L. 2012. Focal electrical intracerebral stimulation of a face-sensitive area causes transient prosopagnosia. *Neuroscience*. 222:281–288.
- Jonas J, Jacques C, Liu-Shuang J, Brissart H, Colnat-Coulbois S, Maillard L, Rossion B. 2016. A face-selective ventral occipito-temporal map of the human brain with intracerebral potentials. *Proc Natl Acad Sci U S A*. 113:4088–4097.
- Jonas J, Rossion B. 2021. Intracerebral electrical stimulation to understand the neural basis of human face identity recognition. *Eur J Neurosci*. 54:4197–4211.
- Jonas J, Rossion B. 2023. Chapter 39 - What are the contributions and challenges of direct intracranial electrical stimulation in human cognitive neuroscience? In: Axmacher N, editor. *Intracranial EEG: a guide for cognitive neuroscientists*. Springer Cham.
- Jonas J, Rossion B, Brissart H, Frismand S, Jacques C, Hossu G, Colnat-Coulbois S, Vespignani H, Vignal J-P, Maillard L. 2015. Beyond the core face-processing network: Intracerebral stimulation of a face-selective area in the right anterior fusiform gyrus elicits transient prosopagnosia. *Cortex*. 72:140–155.
- Jonas J, Rossion B, Krieg J, Koessler L, Colnat-Coulbois S, Vespignani H, Jacques C, Vignal J-P, Brissart H, Maillard L. 2014. Intracerebral electrical stimulation of a face-selective area in the right inferior occipital cortex impairs individual face discrimination. *NeuroImage*. 99:487–497.
- Kanwisher N, McDermott J, Chun MM. 1997. The fusiform face area: a module in human extrastriate cortex specialized for face perception. *J Neurosci*. 17:4302–4311.
- Kanwisher N, Yovel G. 2006. The fusiform face area: a cortical region specialized for the perception of faces. *Philos Trans R Soc B Biol Sci*. 361:2109–2128.
- Keller CJ, Davidesco I, Megevand P, Lado FA, Malach R, Mehta AD. 2017. Tuning face perception with electrical stimulation of the fusiform gyrus. *Hum Brain Mapp*. 38:2830–2842.
- Kovács G. 2020. Getting to know someone: familiarity, person recognition, and identification in the human brain. *J Cogn Neurosci*. 32:2205–2225.
- Leveroni CL, Seidenberg M, Mayer AR, Mead LA, Binder JR, Rao SM. 2000. Neural systems underlying the recognition of familiar and newly learned faces. *J Neurosci*. 20:878–886.
- Liu-Shuang J, Norcia AM, Rossion B. 2014a. An objective index of individual face discrimination in the right occipito-temporal cortex by means of fast periodic oddball stimulation. *Neuropsychologia*. 52:57–72.
- Liu-Shuang J, Norcia AM, Rossion B. 2014b. An objective index of individual face discrimination in the right occipito-temporal cortex by means of fast periodic oddball stimulation. *Neuropsychologia*. 52:57–72.
- Lochy A, Jacques C, Maillard L, Colnat-Coulbois S, Rossion B, Jonas J. 2018. Selective visual representation of letters and words in the left ventral occipito-temporal cortex with intracerebral recordings. *Proc Natl Acad Sci*. 115:7595–7604.
- Mandonnet E, Winkler PA, Duffau H. 2010. Direct electrical stimulation as an input gate into brain functional networks: principles, advantages and limitations. *Acta Neurochir (Wien)*. 152:185–193.
- Mazard A, Schiltz C, Rossion B. 2006. Recovery from adaptation to facial identity is larger for upright than inverted faces in the human occipito-temporal cortex. *Neuropsychologia*. 44:912–922.
- Meadows JC. 1974. The anatomical basis of prosopagnosia. *J Neurol Neurosurg Psychiatry*. 37:489–501.

- Moeller S, Freiwald WA, Tsao DY. 2008. Patches with links: a unified system for processing faces in the macaque temporal lobe. *Science*. 320:1355–1359.
- Mundel T, Milton JG, Dimitrov A, Wilson HW, Pelizzari C, Ufring S, Torres I, Erickson RK, Spire J-P, Towle VL. 2003. Transient inability to distinguish between faces: electrophysiologic studies. *J Clin Neurophysiol Off Publ Am Electroencephalogr Soc*. 20:102–110.
- Natu V, O'Toole AJ. 2011. The neural processing of familiar and unfamiliar faces: A review and synopsis. *Br J Psychol*. 102:726–747.
- Natu VS, O'Toole AJ. 2015. Spatiotemporal changes in neural response patterns to faces varying in visual familiarity. *NeuroImage*. 108:151–159.
- Nestor A, Plaut DC, Behrmann M. 2011. Unraveling the distributed neural code of facial identity through spatiotemporal pattern analysis. *Proc Natl Acad Sci U S A*. 108:9998–10003.
- Niessing J, Ebisch B, Schmidt KE, Niessing M, Singer W, Galuske RAW. 2005. Hemodynamic signals correlate tightly with synchronized gamma oscillations. *Science*. 309:948–951.
- Norcia AM, Appelbaum LG, Ales JM, Cottureau BR, Rossion B. 2015. The steady-state visual evoked potential in vision research: A review. *J Vis*. 15:4.
- Parvizi J, Jacques C, Foster BL, Withoft N, Rangarajan V, Weiner KS, Grill-Spector K. 2012. Electrical stimulation of human fusiform face-selective regions distorts face perception. *J Neurosci*. 32:14915–14920.
- Perrone-Bertolotti M, Alexandre S, Jobb A-S, De Palma L, Baciù M, Mairesse M-P, Hoffmann D, Minotti L, Kahane P, David O. 2020. Probabilistic mapping of language networks from high frequency activity induced by direct electrical stimulation. *Hum Brain Mapp*. 41:4113–4126.
- Puce A, Allison T, McCarthy G. 1999. Electrophysiological studies of human face perception. III: Effects of top-down processing on face-specific potentials. *Cereb Cortex*. 9:445–458.
- Quiroga RQ, Boscaglia M, Jonas J, Rey HG, Yan X, Maillard L, Colnat-Coulbois S, Koessler L, Rossion B. in press. Single neuron responses underlying face recognition in the human midfusiform face-selective cortex. *Nat Commun*.
- Ramon M, Vizioli L, Liu-Shuang J, Rossion B. 2015. Neural microgenesis of personally familiar face recognition. *Proc Natl Acad Sci U S A*. 112:4835–4844.
- Rangarajan V, Hermes D, Foster BL, Weiner KS, Jacques C, Grill-Spector K, Parvizi J. 2014. Electrical stimulation of the left and right human fusiform gyrus causes different effects in conscious face perception. *J Neurosci*. 34:12828–12836.
- Rectem D, Poitrenaud J, Coyette F, Kalafat M, Van der Linden M. 2004. Une épreuve de rappel libre à 15 items avec remémoration sélective (RLS-15). *Solal*.
- Retter TL, Rossion B. 2016. Uncovering the neural magnitude and spatio-temporal dynamics of natural image categorization in a fast visual stream. *Neuropsychologia*. 91:9–28.
- Retter TL, Rossion B, Schiltz C. 2021. Harmonic amplitude summation for frequency-tagging analysis. *J Cogn Neurosci*. 33:2372–2393.
- Ritaccio AL, Brunner P, Schalk G. 2018. Electrical stimulation mapping of the brain: Basic principles and emerging alternatives. *J Clin Neurophysiol Off Publ Am Electroencephalogr Soc*. 35:86–97.
- Rolston JD, Chang EF. 2018. Critical language areas show increased functional connectivity in human cortex. *Cereb Cortex*. 28:4161–4168.

- Rossion B. 2014. Understanding face perception by means of prosopagnosia and neuroimaging. *Front Biosci.* 6:258–307.
- Rossion B. 2022. Twenty years of investigation with the case of prosopagnosia PS to understand human face identity recognition. Part I: Function. *Neuropsychologia.* 173:108278.
- Rossion B, Caldara R, Seghier M, Schuller A-M, Lazeyras F, Mayer E. 2003. A network of occipito-temporal face-sensitive areas besides the right middle fusiform gyrus is necessary for normal face processing. *Brain.* 126:2381–2395.
- Rossion B, Hanseeuw B, Dricot L. 2012. Defining face perception areas in the human brain: A large-scale factorial fMRI face localizer analysis. *Brain Cogn.* 79:138–157.
- Rossion B, Jacques C, Jonas J. 2018. Mapping face categorization in the human ventral occipitotemporal cortex with direct neural intracranial recordings. *Ann N Y Acad Sci.* 1426:5–24.
- Rossion B, Michel C. 2018. Normative accuracy and response time data for the computerized Benton Facial Recognition Test (BFRT-c). *Behav Res Methods.* 50:2442–2460.
- Rossion B, Retter TL, Liu-Shuang J. 2020. Understanding human individuation of unfamiliar faces with oddball fast periodic visual stimulation and electroencephalography. *Eur J Neurosci.* 52:4283–4344.
- Rossion B, Schiltz C, Crommelinck M. 2003. The functionally defined right occipital and fusiform “face areas” discriminate novel from visually familiar faces. *NeuroImage.* 19:877–883.
- Rossion B, Torfs K, Jacques C, Liu-Shuang J. 2015. Fast periodic presentation of natural images reveals a robust face-selective electrophysiological response in the human brain. *J Vis.* 15:1–18.
- Rostalski S-M, Amado C, Kovács G, Feuerriegel D. 2020. Measures of repetition suppression in the fusiform face area are inflated by co-occurring effects of statistically learned visual associations. *Cortex.* 131:123–136.
- Salado AL, Koessler L, De Mijolla G, Schmitt E, Vignal J-P, Civit T, Tyvaert L, Jonas J, Maillard LG, Colnat-Coulbois S. 2017. sEEG is a safe procedure for a comprehensive anatomic exploration of the insula: a retrospective study of 108 procedures representing 254 transopercular insular electrodes. *Oper Neurosurg.* 14:1–8.
- Sanada T, Kapeller C, Jordan M, Grünwald J, Mitsuhashi T, Ogawa H, Anei R, Guger C. 2021. Multi-modal mapping of the face selective ventral temporal cortex – a group study with clinical implications for ECS, ECoG, and fMRI. *Front Hum Neurosci.* 15.
- Schalk G, Kapeller C, Guger C, Ogawa H, Hiroshima S, Lafer-Sousa R, Saygin ZM, Kamada K, Kanwisher N. 2017. Facephenes and rainbows: Causal evidence for functional and anatomical specificity of face and color processing in the human brain. *Proc Natl Acad Sci.* 114:12285–12290.
- Schiltz C, Dricot L, Goebel R, Rossion B. 2010. Holistic perception of individual faces in the right middle fusiform gyrus as evidenced by the composite face illusion. *J Vis.* 10:25.
- Schiltz C, Rossion B. 2006. Faces are represented holistically in the human occipito-temporal cortex. *NeuroImage.* 32:1385–1394.
- Schiltz C, Sorger B, Caldara R, Ahmed F, Mayer E, Goebel R, Rossion B. 2006. Impaired face discrimination in acquired prosopagnosia is associated with abnormal response to individual faces in the right middle fusiform gyrus. *Cereb Cortex.* 16:574–586.

- Schrouff J, Raccach O, Baek S, Rangarajan V, Salehi S, Mourão-Miranda J, Helili Z, Daitch AL, Parvizi J. 2020. Fast temporal dynamics and causal relevance of face processing in the human temporal cortex. *Nat Commun.* 11:656.
- Sergent J, Ohta S, MacDonald B. 1992. Functional neuroanatomy of face and object processing: A positron emission tomography study. *Brain.* 115:15–36.
- Sergent J, Signoret J-L. 1992. Varieties of functional deficits in prosopagnosia. *Cereb Cortex.* 2:375–388.
- Seron X, Mataigne F, Coyette F, Rectem D, Bruyer R, Laterre EC. 1995. [A case of metamorphopsia restricted to faces and different familiar objects]. *Rev Neurol (Paris).* 151:691–698.
- So EL, Alwaki A. 2018. A guide for cortical electrical stimulation mapping: *J Clin Neurophysiol.* 35:98–105.
- Sorger B, Goebel R, Schiltz C, Rossion B. 2007. Understanding the functional neuroanatomy of acquired prosopagnosia. *NeuroImage.* 35:836–852.
- Steeves J, Dricot L, Goltz HC, Sorger B, Peters J, Milner AD, Goodale MA, Goebel R, Rossion B. 2009. Abnormal face identity coding in the middle fusiform gyrus of two brain-damaged prosopagnosic patients. *Neuropsychologia.* 47:2584–2592.
- Talairach J, Bancaud J. 1973. Stereotaxic approach to epilepsy: methodology of anatomofunctional stereotaxic investigations. *Prog Neurol Surg.* 5:297–354.
- Tolias AS, Sultan F, Augath M, Oeltermann A, Tehovnik EJ, Schiller PH, Logothetis NK. 2005. Mapping cortical activity elicited with electrical microstimulation using fMRI in the macaque. *Neuron.* 48:901–911.
- Tranel D, Vianna E, Manzel K, Damasio H, Grabowski T. 2009. Neuroanatomical correlates of the Benton facial recognition test and judgment of line orientation test. *J Clin Exp Neuropsychol.* 31:219–233.
- Trébuchon A, Chauvel P. 2016. Electrical stimulation for seizure induction and functional mapping in stereoelectroencephalography. *J Clin Neurophysiol.* 33:511–521.
- Tsantani M, Kriegeskorte N, Storrs K, Williams AL, McGettigan C, Garrido L. 2021. FFA and OFA encode distinct types of face identity information. *J Neurosci.* 41:1952–1969.
- Volfart A, Yan X, Maillard L, Colnat-Coulbois S, Hossu G, Rossion B, Jonas J. 2022. Intracerebral electrical stimulation of the right anterior fusiform gyrus impairs human face identity recognition. *NeuroImage.* 250:118932.
- Wandell BA. 2011. The neurobiological basis of seeing words. *Ann N Y Acad Sci.* 1224:63–80.
- Wechsler D. 2008. Wechsler adult intelligence scale—Fourth Edition (WAIS—IV). San Antonio, TX: Pearson.
- Weiner KS, Golarai G, Caspers J, Chuapoco MR, Mohlberg H, Zilles K, Amunts K, Grill-Spector K. 2014. The mid-fusiform sulcus: A landmark identifying both cytoarchitectonic and functional divisions of human ventral temporal cortex. *NeuroImage.* 84:453–465.
- Weiner KS, Grill-Spector K. 2012. The improbable simplicity of the fusiform face area. *Trends Cogn Sci.* 16:251–254.
- Yovel G, Kanwisher N. 2005. The neural basis of the behavioral face-inversion effect. *Curr Biol.* 15:2256–2262.
- Zhang J, Li X, Song Y, Liu J. 2012. The fusiform face area is engaged in holistic, not parts-based, representation of faces. *PLOS ONE.* 7:e40390.

- Zhen Z, Yang Z, Huang L, Kong X, Wang X, Dang X, Huang Y, Song Y, Liu J. 2015. Quantifying interindividual variability and asymmetry of face-selective regions: A probabilistic functional atlas. *NeuroImage*. 113:13–25.
- Zhou G, Liu J, Xiao NG, Wu SJ, Li H, Lee K. 2018. The fusiform face area plays a greater role in holistic processing for own-race faces than other-race faces. *Front Hum Neurosci*. 12.
- Zimmermann FGS, Yan X, Rossion B. 2019. An objective, sensitive and ecologically valid neural measure of rapid human individual face recognition. *R Soc Open Sci*. 6:181904.